HHS Public Access

Author manuscript

Cell Rep. Author manuscript; available in PMC 2020 July 02.

Published in final edited form as:

Cell Rep. 2020 March 03; 30(9): 2989–3003.e6. doi:10.1016/j.celrep.2020.02.040.

Innate Lymphoid Cells Play a Pathogenic Role in Pericarditis

Hee Sun Choi[1], **Taejoon Won**[1], **Xuezhou Hou**[2], **Guobao Chen**[1], **William Bracamonte-Baran**[1], **Monica V. Talor**[1], **Ivana Jurčová**[3], **Ondrej Szárszoi**[4], **Lenka Čurnova**[5], **Ilja Stříž**[5], **Jody E. Hooper**[1], **Vojtěch Melenovský**[3], **Daniela Čiháková**[1,2,6,*]

[1]Department of Pathology, School of Medicine, Johns Hopkins University, Baltimore, MD 21205, USA

[2]W. Harry Feinstone Department of Molecular Microbiology and Immunology, Bloomberg School of Public Health, Johns Hopkins University, Baltimore, MD 21205, USA

[3]Department of Cardiology, Institute for Clinical and Experimental Medicine (IKEM), Prague, Czech Republic

[4]Department of Cardiovascular Surgery, Institute for Clinical and Experimental Medicine (IKEM), Prague, Czech Republic

[5]Department of Clinical and Transplant Immunology, Institute for Clinical and Experimental Medicine (IKEM), Prague, Czech Republic

[6]Lead Contact

SUMMARY

We find that cardiac group 2 innate lymphoid cells (ILC2s) are essential for the development of IL-33-induced eosinophilic pericarditis. We show a pathogenic role for ILC2s in cardiac inflammation, in which ILC2s activated by IL-33 drive the development of eosinophilic pericarditis in collaboration with cardiac fibroblasts. ILCs, not T and B cells, are required for the development of pericarditis. ILC2s transferred to the heart of *Rag2*$^{-/-}$*Il2rg*$^{-/-}$ mice restore their susceptibility to eosinophil infiltration. Moreover, ILC2s direct cardiac fibroblasts to produce eotaxin-1. We also find that eosinophils reside in the mediastinal cavity and that eosinophils transferred to the mediastinal cavity of eosinophil-deficient ΔdblGATA1 mice following IL-33 treatment migrate to the heart. Thus, the serous cavities may serve as a reservoir of cardiac-infiltrating eosinophils. In humans, patients with pericarditis show higher amounts of ILCs in pericardial fluid than do healthy controls and patients with other cardiac diseases. We demonstrate that ILCs play a critical role in pericarditis.

*Correspondence: cihakova@jhmi.edu.

AUTHOR CONTRIBUTIONS

H.S.C. and T.W. performed the experiments and analyzed the data. X.H., G.C., W.B.-B., and M.V.T. performed the experiments. I.J., O.S., L.C., I.S., and V.M. obtained the human pericardial fluid and isolated cells. J.E.H. obtained the research autopsy samples of pericardial fluid. H.S.C. and D.C. conceived the main ideas, designed the experiments, interpreted the data and wrote the manuscript. D.C. acquired the funding.

DECLARATION OF INTERESTS

The authors declare no competing interests.

SUPPLEMENTAL INFORMATION

Supplemental Information can be found online at https://doi.org/10.1016/j.celrep.2020.02.040.

Graphical Abstract

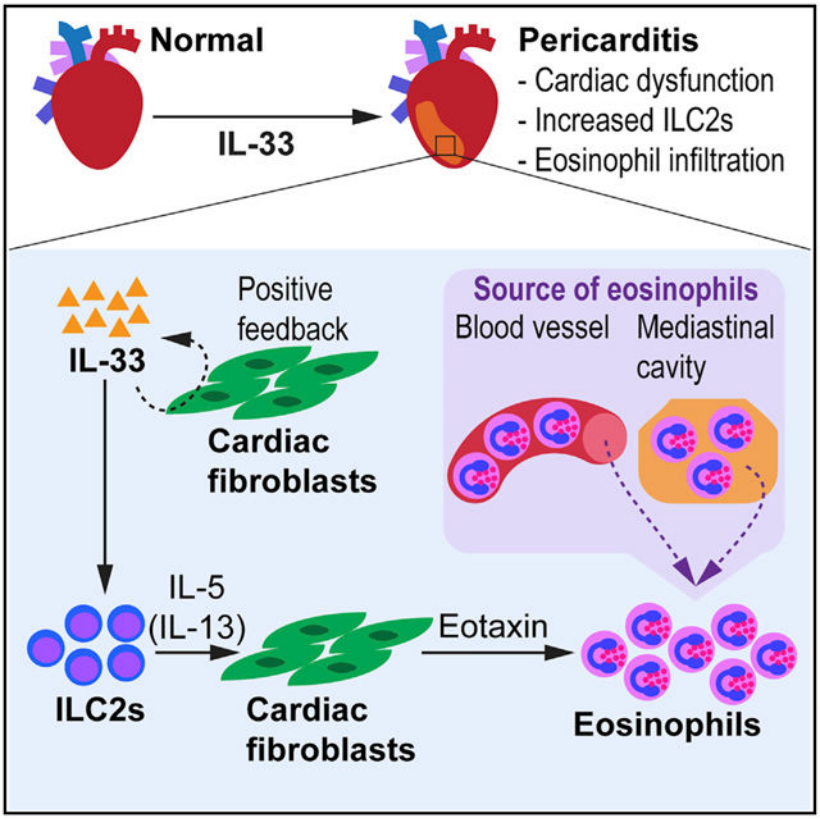

In Brief

Choi et al. show a pathogenic role for innate lymphoid cells (ILCs) in IL-33-induced eosinophilic pericarditis. ILCs are required for the development of pericarditis, and group 2 ILCs (ILC2s) promote the expression of eotaxin by cardiac fibroblasts. In humans, ILCs are found higher in the pericardial fluid of patients with pericarditis compared to others.

INTRODUCTION

Innate lymphoid cells (ILCs) are recently identified innate immune cells that serve important roles in lymphoid tissue formation, repair of damaged tissues, and homeostasis, as well as in immunity against infectious microorganisms (Spits and Cupedo, 2012; Eberl et al., 2015; Klose and Artis, 2016). ILCs are categorized into three groups based on their unique expression of transcription factors, surface markers, and the production of effector cytokines (Spits et al., 2013; Walker et al., 2013). ILC1s are characterized by interferon gamma (IFNγ) production and ILC2s by interleukin-5 (IL-5) and IL-13, while ILC3s are characterized by IL-17 and IL-22. Natural killer (NK) cells are considered a cytotoxic subset of ILC1s (Spits et al., 2013). Distinct from adaptive immune cells such as T cells and B cells, ILCs do not possess antigen-specific receptors (Spits and Cupedo, 2012). ILCs appear to be tissue resident cells and are maintained mostly by selfrenewal in homeostatic settings (Gasteiger et al., 2015; Moro et al., 2016). We recently found that cardiac ILCs are also a

resident population that are type 2-skewed in both human and mouse hearts (Bracamonte-Baran et al., 2019). However, what roles cardiac ILCs play in inflammation are poorly understood.

ILC2s are found in many organs at steady state, including lung and mucosal tissues, and can be activated by IL-33, IL-25, and thymic stromal lymphopoietin (TSLP) (Kim and Artis, 2015; Klose and Artis, 2016; Moro et al., 2010; Neill et al., 2010; Price et al., 2010; Kim et al., 2013). After activation, ILC2s produce T helper 2 cell (Th2)-associated cytokines, such as IL-5 and IL-13 (Moro et al., 2010; Neill et al., 2010; Price et al., 2010). These Th2 cytokines have been implicated in eosinophil proliferation, recruitment, and homeostasis (Nussbaum et al., 2013; Price et al., 2010). The role of ILC2s in infection and inflammation has been investigated mostly in mucosa-associated tissues and skin. ILC2s are beneficial in promoting immunity to parasite infection with *Nippostrongylus brasiliensis* (Moro et al., 2010; Neill et al., 2010). In this helminth infection model, IL-25 and IL-33 were shown to be critical for ILC2 activation, and IL-13 produced by ILC2s mediated worm expulsion (Neill et al., 2010). In contrast to the protective immunity provided by ILC2s, IL-33-activated ILC2s are also involved in the pathogenesis of asthma and atopic dermatitis promoting inflammation in the lungs and skin, respectively (Halim et al., 2012; Salimi et al., 2013; Imai et al., 2013). Moreover, the enrichment of ILC2s was reported in biopsy samples from patients with eosinophilic esophagitis and atopic dermatitis (Doherty et al., 2015; Salimi et al., 2013).

IL-33 is a cytokine of the IL-1 family and functions as an alarmin, which is released from cells upon tissue damage or cellular stress (Schmitz et al., 2005; Cayrol and Girard, 2014; Molofsky et al., 2015). IL-33 is usually expressed and released from epithelial and endothelial cells, and it is also shown to be expressed in stromal cells such as fibroblastic reticular cells in the lymph nodes (Moussion et al., 2008; Pichery et al., 2012). The profiling of IL-33 mRNA expression in mouse tissues revealed that the heart had a relatively low expression of IL-33 compared to mucosal and barrier-related tissues such as lung and skin (Schmitz et al., 2005). The role of IL-33 in the heart has been shown to be beneficial in some mouse models of cardiovascular diseases. IL-33 treatment reduced cardiac hypertrophy in a mouse model of transverse aortic constriction and improved cardiac function and survival in a myocardial infarction mouse model (Sanada et al., 2007; Chen et al., 2015; Seki et al., 2009). However, the administration of IL-33 induced pericarditis in mice with an increased proportion of eosinophils in the heart of naive and coxsackievirus B3 (CVB3)-infected mice, demonstrating that IL-33 can also play a pathogenic role in the heart (Abston et al., 2012). IL-33 has been shown to activate and expand ILC2s (Moro et al., 2010; Neill et al., 2010; von Moltke and Locksley, 2014; Kim and Artis, 2015). This suggests that the described pathogenic effect of IL-33 in the heart could be mediated by the activation of ILC2s.

Here, we show that ILCs in the heart play a pathogenic role in promoting cardiac inflammation. Cardiac ILC2s activated by IL-33 caused eosinophilic pericarditis. The IL-33-ST2 signaling axis was important for the expansion of cardiac ILC2s and induction of pericarditis. We identified that ILCs, not T cells and B cells, were required for IL-33-induced pericarditis. *Rag2*$^{-/-}$*Il2rg*$^{-/-}$ mice deficient in lymphocytes, including ILCs, were protected from pericarditis; however, ILC2 transfer to the heart restored the susceptibility of

Rag2$^{-/-}$ *Il2rg*$^{-/-}$ mice to eosinophil infiltration to the heart. We also found that ILC2s induced cardiac fibroblasts to produce eotaxin-1 to direct eosinophil trafficking to the heart. Moreover, we discovered that eosinophils resided in the mediastinal cavity of naive mice, which serves as a reservoir of eosinophils. We documented the recruitment of eosinophils from the mediastinal cavity, which could be an alternate route in addition to the conventional vascular trafficking of eosinophils to the heart. Finally, we showed that, in humans, ILCs are found more frequently in pericardial fluid from pericarditis patients compared to individuals without cardiac diseases and patients with other types of cardiac diseases.

RESULTS

Number of ILC2s Increases in the Heart after IL-33 Treatment

ILC2s express the IL-33 receptor, which is also known as ST2, and become activated and proliferative upon IL-33 stimulation (Spits et al., 2013; Walker et al., 2013; Klose and Artis, 2016). To determine whether IL-33 induces an increase in ILC2s in the heart *in vivo*, we used the IL-33-induced pericarditis model in which mice are treated with IL-33 intraperitoneally every other day for 9 days (Abston et al., 2012). IL-33-treated mice developed severe pericarditis compared to PBS-treated mice (Figure 1A). The inflammation mostly affected the pericardium; however, in some cases, the adjacent myocardium was also inflamed (Figure 1A). We also found that IL-33-treated mice showed an increased infiltration of immune cells in other organs including esophagus and lungs (Figures S1A and S1B). We assessed cardiac function of the heart by performing M-mode and Doppler echocardiography. A typical pattern of ventricular dilation was present in IL-33-treated mice examined by M-mode echocardiography (Figure 1B). IL-33 treatment resulted in reduced ejection fraction (EF) and fractional shortening (FS) (Figures 1C and 1D). Other parameters were comparable; however, the left ventricular posterior wall at end-systole was thinner in IL-33-treated mice (Figures S1C-S1E). In addition, IL-33-treated mice showed significantly longer isovolumetric relaxation time (IVRT), an indicator of diastolic function, and higher myocardial performance index (MPI), a useful predictor of global cardiac function, than PBS-treated mice (Figures 1E and 1F). Prolonged IVRT indicates poor myocardial relaxation related to pericardial constriction, and high MPI represents both systolic and diastolic dysfunction. These data suggest that pericarditis induced by IL-33 resulted in abnormal cardiac function. We analyzed the number of heart-infiltrating CD45^{+} leukocytes by flow cytometry and found that it was significantly increased in IL-33-treated mice compared to PBS-treated mice, confirming that inflammation occurred in the heart as a result of IL-33 treatment (Figure 1G). We identified ILC2s in the heart as CD45^{+}Lin^{-}CD90^{+}KLRG1^{+}ST2^{+} (Figure S2A). Lin included CD3ε, TCRβ, CD19, B220, CD11b, CD11c, Gr-1, Ter119, FcεRIα, and NKp46, and was used to exclude cell populations that may contaminate ILC2s. Both the number and frequency of ILC2s in the heart were dramatically increased upon IL-33 treatment compared to PBS treatment (Figures 1H and S2B). We also analyzed other heart-infiltrating immune cells and found that the number and frequency of CD11b^{+}SiglecF^{+} eosinophils were increased in the heart of IL-33-treated mice and that they were the most abundant cells among heart infiltrates (Figures 1I and S2C). The number and frequency of other immune cells known to express ST2, including FcεRIα^{+}CD117(c-Kit)$^{+}$ mast cells, remained unchanged (Figure 1J). To visualize the distribution of

ILC2s and eosinophils in pericarditis, we used a tissue-clearing technique with the right ventricle of the heart from mice treated with IL-33. We found that ILC2s and eosinophils were located in the right ventricle near the pericardium and in the atria, which is consistent with the finding that inflammation was mostly observed in the right ventricle in the histological analysis (Figure 1K; Video S1). In addition, the number of $CD11b^{+}Ly6G^{+}$ neutrophils in the heart was decreased in IL-33-treated mice; however, we did not find significant changes in numbers of macrophages, monocytes, T cells, B cells, and NK cells (Figures S2D-S1I). We found that the level of anti-myosin immunoglobulin M (IgM) antibody in serum was significantly higher in IL-33-treated mice than in PBS-treated mice on day 9 (Figure S2J). Anti-myosin IgG and IgE were found at a negligible level in the sera of both PBS- and IL-33-treated mice (data not shown). These results indicate that IL-33-induced pericarditis is characterized by impaired cardiac function and an increased number of ILC2s and eosinophilsin the heart.

IL-33-ST2 Signaling Pathway Is Critical for ILC Accumulation in the Heart and the Development of Pericarditis

To determine whether the development of pericarditis is dependent on the IL-33-ST2 signaling pathway, $ST2^{-/-}$ (*Il1rl1*$^{-/-}$) mice were treated with IL-33. $ST2^{-/-}$ mice were completely protected from the development of IL-33-induced pericarditis, whereas wild-type (WT) mice developed pericarditis (Figures 2A and 2B). The number of total leukocyte infiltrates was significantly reduced in the heart of $ST2^{-/-}$ mice compared to WT mice (Figure 2C). To further confirm the dependency of ILC2 accumulation in the heart on IL-33 signaling, we analyzed the $Lin^{-}CD90^{+}KLRG1^{+}$ ILC population in the heart of $ST2^{-/-}$ mice after IL-33 treatment. We found that ILCs were significantly reduced in the heart of $ST2^{-/-}$ mice compared to WT mice (Figures 2D and 2E). The number of eosinophils was also decreased in the heart of $ST2^{-/-}$ mice (Figure 2F). This demonstrates that IL-33 signaling through ST2 is important for the development of pericarditis, and the IL-33-ST2 signaling axis is required for ILC2 accumulation in the heart. Next, we assessed whether exogenous IL-33 treatment is involved in a positive feedback loop that results in increased endogenous expression of IL-33. IL-$33^{cit/+}$ reporter mice treated with IL-33 showed a higher expression of IL-33 compared to mice treated with PBS, which indicates the presence of a positive feedback loop of IL-33 expression (Figures 2G and S3A). In addition, the number of IL-33-expressing cells was increased after IL-33 treatment (Figure 2H). Most of the IL-33-expressing cells were $CD45^{-}CD31^{-}$ stromal cells, and among them, $Sca1^{+}$ fibroblasts were the major IL-33-expressing cells in the heart. These IL-33-expressing cardiac fibroblasts were increased in number after IL-33 treatment, suggesting that cardiac fibroblasts have a capacity to produce IL-33 in both the naive state and during cardiac inflammation (Figures 2I and 2J). $Sca1^{+}$ cardiac fibroblasts also expressed platelet-derived growth factor receptor α (PDGFRα), a commonly used cardiac fibroblast marker (Figure 2K). Moreover, we found that IL-33 was spatially expressed by cardiac fibroblasts near and in the pericardium (Figure 2L). We found a correlation of IL-33 and ST2 expression in IL-33-induced pericarditis, indicating the existence of a positive feedback loop in which IL-33 induces greater ST2 expression and IL-33 production by fibroblasts (Figure S3B). Furthermore, we examined whether endogenous IL-33 is important to induce pericarditis. We found that the number of total $CD45^{+}$ heart-infiltrating leukocytes was reduced in IL-$33^{-/-}$ mice compared to WT

mice upon IL-33 treatment (Figure S3C). The number of myeloid cells and eosinophils was also decreased in the heart of IL-33$^{-/-}$ mice (Figures S3D and S3E). The lack of endogenous IL-33 affected the Lin^{-}CD90^{+}KLRG1^{+} ILC population, which was reduced in the heart of IL-33$^{-/-}$ mice compared to WT mice (Figure S3F). These results indicate that endogenous IL-33 is a required component to induce severe pericarditis, which was initiated by exogenous IL-33 administration. These data suggest that IL-33 signaling through ST2 is important for ILC accumulation in the heart and the development of pericarditis.

ILCs Are Required for Development of IL-33-Induced Pericarditis and Sufficient to Rescue ILC-Deficient Mice Susceptibility to Eosinophil Infiltration

To determine whether ILCs are required for the induction of pericarditis, we treated WT, *Rag2*$^{-/-}$, and *Rag2*$^{-/-}$*Il2rg*$^{-/-}$ mice with IL-33. While *Rag2*$^{-/-}$ mice deficient in T cells and B cells developed pericarditis comparable to WT mice, *Rag2*$^{-/-}$*Il2rg*$^{-/-}$ mice, which lack all lymphocytes including ILCs, were completely protected from the development of pericarditis (Figures 3A and 3B). Thus, adaptive immune response is not necessary for the induction of pericarditis by IL-33. We assessed leukocytes in the heart and found a significantly reduced number of CD45^{+} cells in the heart of *Rag2*$^{-/-}$*Il2rg*$^{-/-}$ mice compared to both WT and *Rag2*$^{-/-}$ mice (Figure 3C). ILC2s were increased in the heart of WT and *Rag2*$^{-/-}$ mice treated with IL-33, whereas ILC2s were not found in the heart of *Rag2*$^{-/-}$*Il2rg*$^{-/-}$ mice (Figure 3D). IL-33-treated *Rag2*$^{-/-}$*Il2rg*$^{-/-}$ mice showed a smaller number of eosinophils, but more neutrophils in the heart than WT and *Rag2*$^{-/-}$ mice (Figures 3E and S4A). These data suggest that ILCs are required for the development of pericarditis induced by IL-33, and adaptive immune cells such as T and B cells may not be involved in the pathogenesis of IL-33-induced pericarditis. To confirm that IL-33-induced pericarditis is ILC2-dependent, we investigated the ability of transferred ILC2s to reverse the resistance of *Rag2*$^{-/-}$*Il2rg*$^{-/-}$ mice to pericarditis development. We performed fluorescence-activated cell sorting (FACS) to isolate CD45^{+}Lin^{-}CD90^{+} KLRG1^{+}ST2^{+} ILC2s from the hearts of CD45.1^{+} WT donor mice after IL-33 treatment (Figure S4B). Intravenous transfer of ILC2s was not successful, and we were not able to detect any transferred ILC2s in the heart of recipient mice, which is consistent with the resident status of ILCs and their inability to traffic to the heart from the blood, as we showed before (Bracamonte-Baran et al., 2019). Therefore, we expanded FACS-sorted CD45.1^{+} ILC2s *in vitro* and injected them directly into the myocardium of ILC-deficient CD45.2^{+} *Rag2*$^{-/-}$*Il2rg*$^{-/-}$ recipient mice followed by IL-33 treatment (Figure S4C). Recipient mice in a control group were injected with media in the myocardium followed by IL-33 treatment. We were able to detect CD45.1^{+} ILC2s in the hearts of ILC2-transferred CD45.2^{+} *Rag2*$^{-/-}$*Il2rg*$^{-/-}$ mice on day 9, indicating that ILC2s injected into the myocardium remained for the course of the disease (Figure 3F). The number of heart-infiltrating CD45.2^{+} leukocytes was increased in *Rag2*$^{-/-}$*Il2rg*$^{-/-}$ mice injected with ILC2s compared to mice injected with media (Figure 3G). Eosinophils were significantly increased in the hearts of *Rag2*$^{-/-}$*Il2rg*$^{-/-}$ mice injected with ILC2s compared to mice injected with media, providing evidence of a critical role for cardiac ILC2s in eosinophil recruitment to the heart during the development of pericarditis (Figures 3H and 3I). To summarize, ILCs, but not T cells and B cells, are required for the development of pericarditis, and the adoptive transfer of cardiac ILC2s directly to the heart is sufficient to

rescue *Rag2*$^{-/-}$*Il2rg*$^{-/-}$ mice susceptibility to eosinophilic cardiac inflammation induced by IL-33.

ILC2s Drive Cardiac Fibroblasts to Upregulate CCL11/Eotaxin-1 Gene Expression

Eotaxin production is known to induce eosinophil trafficking into organs following a chemoattractant gradient (Rothenberg, 1999; Borchers et al., 2002). We previously found that the eotaxin-CCR3 pathway is the main mechanism for eosinophil trafficking to the heart (Diny et al., 2016). We found that the expression of *Ccl11*, a gene encoding eotaxin-1, was upregulated in the heart of IL-33-treated mice compared to PBS-treated mice, while the expression of *Ccl24* encoding eotaxin-2 was comparable between groups (Figures 4A and S5A). Our previous work showed that cardiac fibroblasts produce a diverse set of cytokines and chemokines in response to different Th environments (Chen et al., 2018). Specifically, in a Th2 environment during eosinophilic cardiac inflammation, cardiac fibroblasts are the main source of eotaxin-1 (Diny et al., 2016). To investigate whether ILC2s and cardiac fibroblasts cooperate to attract eosinophils to the heart in IL-33-induced pericarditis, we devised a co-culture system in which cardiac fibroblasts are co-cultured with ILC2s separated by 0.4-μm transwells (Figure 4B). This enabled ILC2s to interact with cardiac fibroblasts through soluble factors such as cytokines, but not through direct contact. We found that cardiac fibroblasts significantly upregulated *Ccl11* expression when co-cultured with ILC2s in the presence of IL-33, compared to cardiac fibroblasts cultured without ILC2s in the absence or presence of IL-33 (Figure 4C). *Ccl24* expression by cardiac fibroblasts did not significantly differ (Figure S5B). Eotaxin-1 concentration in the cell culture supernatant was also significantly increased in the co-culture condition in which cardiac fibroblasts are cultured with ILC2s in the presence of IL-33 (Figure 4D). To determine whether ILC2s are required for increased eotaxin expression *in vivo*, we examined expression levels of genes related to eosinophil trafficking and ILC2 effector cytokines in the heart of WT, *Rag2*$^{-/-}$, and *Rag2*$^{-/-}$*Il2rg*$^{-/-}$ mice treated with IL-33. We found that the expression of both *Ccl11* and *Ccl24* was significantly decreased in *Rag2*$^{-/-}$*Il2rg*$^{-/-}$ mice compared to WT mice (Figures 4E and 4F). The expression levels of *Il5* and *Il13*, encoding ILC2 effector cytokines, were also downregulated in *Rag2*$^{-/-}$*Il2rg*$^{-/-}$ mice (Figures 4G and 4H). These data suggest that ILCs may be required for eotaxin expression *in vivo*, possibly in an ILC2 effector cytokines-dependent way. We also examined the spatial expression of eotaxin-1 in the heart and found that eotaxin-1 was highly produced near the pericardium, where pericarditis occurs (Figure 4I). In summary, ILC2s are able to stimulate cardiac fibroblasts to produce eotaxin-1 via soluble factors, suggesting a role for ILC2s and cardiac fibroblasts in the recruitment of eosinophils into the heart.

ILC2-Derived IL-5 Affects the Development of IL-33-Induced Pericarditis

We assessed cytokine production by cardiac ILC2s on day 9 post-IL-33 treatment using flow cytometry. We found that ILC2s in the heart produced both IL-5 and IL-13 after IL-33 treatment (Figure 5A). Eighty percent of ILC2s found in the heart produced both IL-5 and IL-13 (Figure 5B). To examine the role of IL-5 in the development of pericarditis, we depleted IL-5 in IL-33-treated mice using an anti-IL-5 monoclonal antibody (mAb). We found that mice injected with IL-5-neutralizing mAb showed a trend of less severe pericarditis by histology after IL-33 administration compared to those injected with isotype

control (Figure 5C). In addition, we found that the total number of leukocytes in the heart was significantly decreased in anti-IL-5-treated mice compared to isotype-treated controls (Figure 5D). Eosinophils were also significantly reduced in the heart of anti-IL-5-treated mice compared to isotype-treated mice (Figure 5E). However, the number of ILC2s was similar between groups (Figure 5F). These data show that IL-5 produced by ILC2s drives eosinophil infiltration to the heart and contributes to the severity of pericarditis. We also examined whether IL-13 plays a role in pericarditis development. IL-13$^{-/-}$ mice showed pericarditis similar to WT mice (Figure 5G). We found the number of total leukocytes and eosinophils were analogous between WT and IL-13$^{-/-}$ mice (Figures 5H and 5I). ILC2s did not differ in number between WT and IL-13$^{-/-}$ mice with pericarditis (Figure 5J). These data suggest that IL-5 derived from ILC2s affects the development of pericarditis and cardiac infiltrating immune cells.

Eosinophils Are Present in the Mediastinal Cavity and Can Migrate to the Heart

Previously, we found that the eotaxin-CCR3 pathway is critical for eosinophil migration to the heart during eosinophilic myocarditis (Diny et al., 2016). We also showed that ILC2s stimulated by IL-33 promote eotaxin-1 production by cardiac fibroblasts (Figures 4C and 4D). However, given that IL-33-induced cardiac inflammation has a unique disease pattern affecting predominantly the pericardium and myopericardium, we wanted to explore whether eosinophils could migrate from a non-vascular source such as the mediastinal cavity, a neighboring serosal cavity. In mice, there are pericardial pores between the pericardial, pleural, and mediastinal cavities (Fukuo et al., 1988). We found that eosinophils resided in the mediastinal cavity of naive WT mice at a frequency comparable to that of eosinophils in the heart (Figures 6A and 6B). To examine whether eosinophils would be present in the mediastinal cavity in higher numbers in hypereosinophilia, we examined eosinophils in the mediastinal cavity of naive IL-5 transgenic (IL-5Tg) mice, which spontaneously develop tissue and blood eosinophilia (Lee et al., 1997). In IL-5Tg mice, we found eosinophils at a high frequency in the mediastinal cavity, as well as in the heart and blood (Figures 6C and 6D). The frequency of neutrophils in the mediastinal cavity of both WT and IL-5Tg mice was significantly lower compared to the frequency in the blood of these mice, indicating that eosinophils found in the mediastinal cavity were not from blood contamination (Figures S6Aand 6B). We found that PBS-treated WT mice had a frequency of eosinophils and neutrophils in the heart, mediastinal cavity, and blood similar to that of naive WT mice (Figures 6B, S6A, S6C, and S6E). Neutrophils in the blood of IL-33-treated WT mice were found to be higher than in the heart and mediastinal cavity, as shown similarly in naive IL-5Tg mice (Figures S6B and S6F). However, in IL-33-treated mice, eosinophils were present at a higher frequency in the heart and mediastinal cavity than in the blood (Figure S6D). To determine whether eosinophils can migrate to the heart from the mediastinal cavity in addition to the vasculature, we transferred the same number of eosinophils either to the mediastinal cavity or intravenously (i.v.) to IL-33-treated ΔdblGATA1 mice lacking eosinophils (Figure 6E). Both mediastinal cavity and i.v. transfers were performed simultaneously to the same animal. The mediastinal cavity transfer was conducted by the direct injection of eosinophils into the mediastinum without an open-chest surgery. Eosinophils injected into the mediastinal cavity and i.v. were labeled with different fluorescent cell-tracking dyes, CellTrace Violet (CTV) and CellTrace Far Red (CTFR),

respectively (Figures 6E and 6F). Eosinophils transferred to the mediastinal cavity were found to remain mostly in the cavity, confirming that the transfer to the cavity was correctly performed (Figure S6G). We found eosinophils transferred through both routes in the heart of ΔdblGATA1 mice deficient in eosinophils (Figures 6G and 6H). Eosinophils transferred to the mediastinal cavity were found at a significantly higher frequency in the heart of ΔdblGATA1 mice compared to eosinophils transferred intravenously (Figures 6H and 6I). This indicates that eosinophils can migrate from the mediastinal cavity to the heart in addition to traditional vascular routes. Thus, we demonstrated that eosinophils are present in the mediastinal cavity and increased in the cavity of IL-33-treated mice or hypereosinophilic mice. We also showed that eosinophils can migrate to the heart from the neighboring serosal cavities. In addition to direct eosinophil supply from the circulation, the mediastinal cavity seems to serve as an eosinophil reservoir, leading to non-vascular eosinophil trafficking to the heart in the IL-33-induced pericarditis model.

ILCs Are Increased in the Pericardial Fluid of Human Pericarditis

To investigate the pathophysiological relevance of ILCs in human pericarditis, we examined whether ILCs are increased in the pericardial fluid from pericarditis patients. We collected pericardial fluid from patients with diverse heart diseases, including pericarditis, and comprehensively profiled immune cells from the pericardial space using high-dimensional mass cytometry (Cy-TOF). Pericardial fluid samples were obtained from patients with arrhythmogenic right ventricular cardiomyopathy (ARVC), ischemic heart disease (IHD), valve disease, or pericarditis during surgical procedures or pericardiocentesis. Pericardial fluid specimens obtained from the rapid autopsy of deceased patients with no cardiovascular diseases served as a control. Most of the alive single cells that were isolated from the human pericardial fluid were $CD45^+$ leukocytes (Figure 7A). To identify ILCs in the pericardial fluid, we excluded myeloid cells and other lymphoid cells such as granulocytes, macrophages, monocytes, dendritic cells, T cells, B cells, and NK cells using cell-specific markers such as CD66b, CD11b, CD68, CD3, CD19, HLA-DR, and CD56 (Figure 7A). ILCs were then defined as $CD127^+$ cells (Figure 7A). We found that, whereas ILCs were a rare population in the pericardial fluid of autopsy controls, the frequency of pericardial ILCs was highly increased in patients with pericarditis compared to controls (Figures 7B and 7C). Although other cardiac disease groups such as ARVC, IHD, and valve disease showed a slightly increasing trend of pericardial ILCs compared to controls, the frequency of ILCs in pericarditis was significantly higher than that in other cardiac diseases (Figures 7B and 7C). Using conventional flow cytometry, we confirmed that Lin^-CD127^+ ILCs were increased in the pericardial fluid from pericarditis patients compared to controls (Figure 7D). These findings suggest that ILCs are a specific population that is increased in the pericardium of patients with pericarditis as we observed in the pericarditis mouse model and that the increase in pericardial fluid ILCs is a unique feature in pericarditis, which is differentiated from other cardiac diseases.

DISCUSSION

We demonstrated that ILC2s accumulate in the heart following IL-33 treatment in mice using a previously described model of IL-33-induced pericarditis (Abston et al., 2012). We

report a pathogenic role for ILC2s in the cardiac inflammation, which implies that cardiac ILC2s activated by IL-33 drive eosinophilic pericarditis in collaboration with cardiac fibroblasts. With advanced visualizing tools using the tissue-clearing technique and light sheet microscopy, we revealed that cardiac ILC2s are located in the ventricles near the pericardium where eosinophilic pericarditis is observed after IL-33 treatment, which supports their role in the development of pericarditis. We identified that ILCs are required for the development of IL-33-induced pericarditis. Given that *Rag2*$^{-/-}$ mice develop comparable cardiac inflammation and pathology to WT mice following IL-33 treatment, we excluded adaptive lymphocytes such as T cells and B cells from being drivers of the development of pericarditis. The necessity of ILC2s in the induction of inflammation has been shown in other organs such as allergen-induced lung inflammation models (Halim et al., 2012; Kim et al., 2012). Papain causes asthma-like symptoms in *Rag1*$^{-/-}$ mice but not in *Rag2*$^{-/-}$*Il2rg*$^{-/-}$ mice, and ILC-deficient *Rag2*$^{-/-}$*Il2rg*$^{-/-}$ mice reconstituted with ILC2s develop airway inflammation (Halim et al., 2012). While *Rag2*$^{-/-}$ mice lack T cells and B cells, *Rag2*$^{-/-}$*Il2rg*$^{-/-}$ mice are deficient in ILCs in addition to T cells and B cells. Unlike *Rag2*$^{-/-}$ mice, *Rag2*$^{-/-}$*Il2rg*$^{-/-}$ mice were protected from IL-33-induced pericarditis, demonstrating that ILCs are required for pericarditis development. Our adoptive transfer experiments showed that cardiac ILC2s transferred directly to the heart of pericarditis-resistant *Rag2*$^{-/-}$*Il2rg*$^{-/-}$ mice elicited cardiac eosinophil infiltration. These findings support the notion that ILCs are tissue resident cells even during acute inflammation as described by us in the heart and others in different organs (Gasteiger et al., 2015; Moro et al., 2016; Bracamonte-Baran et al., 2019). IL-33-treated mice had increased anti-myosin IgM antibody found in their sera, which suggests a possible pathogenic role for ILCs in myopericarditis. ILC2s isolated from the lungs promoted the production of immunoglobulin including IgM by B1 and B2 cells *in vitro* (Drake et al., 2016).

The IL-33-induced pericarditis model allowed us to investigate the pathogenic role of the IL-33-ST2 axis in ILC2 activation during cardiac inflammation. IL-33 mediates its effects through binding to its receptor ST2 as we demonstrated in cardiac ILC2 activation (Schmitz et al., 2005). ST2 is known to be expressed not only on ILC2s but also on Th2 cells, B cells, basophils, eosinophils, dendritic cells, mast cells, and NK T cells (Griesenauer and Paczesny, 2017). However, using an adoptive transfer experiment, we showed that ILC2s are essential for IL-33-induced cardiac inflammation. It was reported that IL-33 expression increases during cardiac inflammation or after cardiac injury, representing an association between IL-33 and its pathological outcome in cardiac inflammation (Chen et al., 2015; Sánchez-Más et al., 2014). ST2 is not only expressed as a membrane-bound form but also produced as a soluble form (soluble ST2 [sST2]) that is released into the circulation. sST2 has been proposed as a prognostic marker for chronic and acute heart failure and aortic stenosis (McCarthy and Januzzi, 2018; Friões et al., 2015; Coronado et al., 2019; Lindman et al., 2015). This is consistent with our findings that the IL-33-ST2 axis plays a key pro-inflammatory role in the heart by stimulating cardiac ILC2s under certain conditions related to increased IL-33 production. It should be noted that IL-33 signaling via ST2 could play a beneficial role in different types of heart disease such as pressure overload and myocardial infarction by providing improved cardiac function and survival (Sanada et al., 2007; Seki et al., 2009).

We showed that IL-33 is expressed in naive heart, and its expression is increased in pericarditis, suggesting its pathogenic role in cardiac inflammation. When mice were treated with exogenous IL-33, its endogenous expression was increased in the heart, thus offering evidence for the presence of a positive feedback loop in the heart. Moreover, IL-33-deficient mice developed less severe inflammation with smaller number of infiltrating leukocytes, including eosinophils compared to WT mice after exogenous IL-33 treatment, which indicates the importance of endogenous IL-33 as a component of the positive feedback loop in the development of pericarditis. Thus, the IL-33-induced pericarditis model does not rely solely on exogenous IL-33 administration, but endogenous IL-33 may contribute to an increased IL-33 level in the heart leading to the development of disease. We identified that $Sca1^+$ cardiac fibroblasts are major producers of IL-33 in the heart, both in steady state and during pericarditis. We previously found that cardiac fibroblasts are a versatile stromal cell type capable of producing different sets of cytokines and chemokines in response to changes in the microenvironment (Chen et al., 2018; Diny et al., 2016). The IL-33-expressing cardiac fibroblasts are located near and in the pericardium, supporting the possible involvement of cardiac fibroblasts in ILC2 activation and pericarditis development through their IL-33 expression. Although it has been reported that endothelial cells or cardiomyocytes could be an important source for IL-33, we did not find mouse endothelial cells to be a major producer of IL-33 in the heart (Pichery et al., 2012; Moussion et al., 2008; Küchler et al., 2008; Demyanets et al., 2013). In our model, we found that cardiac fibroblasts are potent IL-33 producers and increase IL-33 production in response to systemic IL-33 administration, suggesting the existence of a feed-forward loop.

ILC2s produce Th2 cytokines such as IL-5 and IL-13 upon activation with IL-33. We were able to show that IL-33-activated ILC2s induce eotaxin-1 (CCL11) production by cardiac fibroblasts. We previously found that cardiac fibroblasts are the major CCL11 producers in eosinophilic myocarditis mouse model, and CCL11 expression is induced in cardiac fibroblasts *in vitro* in response to IL-4 and IL-13 (Diny et al., 2016). It has been reported that IL-13 potently induces eotaxin expression in lung epithelial cells, esophagus, and other organs (Li et al., 1999; Matsukura et al., 2001; Zuo et al., 2010; Moore et al., 2002; Takahashi et al., 2013; Blanchard et al., 2007). We found, *in vivo*, that cardiac ILC2s are potent producers of IL-13 upon IL-33 activation. Furthermore, cardiac ILC2s are capable of inducing the production of CCL11 by cardiac fibroblast *in vitro*. The expression of eotaxin and type 2 cytokines in the heart was downregulated in ILC-deficient $Rag2^{-/-}Il2rg^{-/-}$ mice compared to WT and $Rag2^{-/-}$ mice, suggesting that eotaxin expression, and subsequent eosinophil recruitment to the heart, may occur in an ILC-dependent way *in vivo*. In addition, eotaxin expression was spatially concentrated in the pericardium and interstitial space, which could explain the specific inflammation pattern of eosinophilic pericarditis induced by IL-33.

We also found that cardiac ILC2s produce IL-5, which plays an important role in developing IL-33-induced pericarditis and that blocking of IL-5 protected mice from the development of eosinophilic pericarditis. In response to IL-5, eosinophils are released into the circulation, which may be hindered by blocking IL-5. Several anti-IL-5 agents, including mepolizumab, reslizumab, and benralizumab, which block IL-5 signaling via IL-5 receptor and reduce blood eosinophils, have been developed, approved, and used to treat asthma in clinical

practice (Farne et al., 2017). In addition, a phase II clinical trial (NCT02130882) is evaluating the safety and efficacy of benralizumap, an anti-IL-5 receptor biologic, in decreasing eosinophils in patients with hypereosinophilic syndrome. We found that anti-IL-5 treatment had a profound effect on reducing eosinophils infiltrating to the heart during pericarditis, suggesting that anti-IL-5/IL-5R agents could be used as a potential treatment for eosinophilic pericarditis.

IL-33-induced cardiac inflammation has a unique pattern affecting mostly pericardium and myopericardium; therefore, we explored whether eosinophils could migrate from a non-vascular source such as the mediastinal cavity, a neighboring serosal cavity. We identified that eosinophils are present in the mediastinal cavity of naive mice and that adoptively transferred eosinophils to the mediastinal cavity of IL-33-treated eosinophil-deficient mice are able to traffic to the heart. This suggests that the serous cavities may serve as a reservoir of cardiac-infiltrating eosinophils. Immune cells have been previously identified in serous cavities such as the peritoneum and pleural cavity (Ha et al., 2006; Shimotakahara et al., 2007; Wang and Kubes, 2016; Weber et al., 2014; Deniset et al., 2019). Macrophages residing in the peritoneal cavity are rapidly recruited to the injured liver through a non-vascular route and display tissue-reparative phenotypes (Wang and Kubes, 2016). Macrophages found in mouse pericardial fluid played a reparative role after myocardial infarction (Deniset et al., 2019). The pleural space is also shown to possess B1a B cells, which can migrate to the lung and produce protective IgM in response to bacterial infection (Weber et al., 2014). We found that eosinophils residing in the mediastinal cavity can migrate to the heart. There are pericardial pores between pericardial, pleural, and mediastinal cavities (Fukuo et al., 1988). Therefore, all of these cavities should be considered a possible source of cells infiltrating to the heart. This does not exclude the contribution of circulating eosinophils to the development of pericarditis; however, it is noteworthy that the mediastinal cavity can serve as an alternative reservoir of eosinophils, which may lead to rapid infiltration during inflammation in close proximity to the heart. IL-33 treatment also induces inflammation in lungs and esophagus, as we demonstrated here and shown before by others (Travers et al., 2017; Judd et al., 2016). After treating mice with IL-33, we found pericardial, subserosal, and peribronchial eosinophil infiltrates in the heart, esophagus, and lungs, respectively. IL-33-induced esophagitis has a subserosal inflammation pattern that is similar to IL-33-induced pericarditis, with the inflammation mostly confined to the subserosa rather than to the mucosa. Based on these observations, we speculate that the chest serosal cavities could also be a source of eosinophils for other organs located in the mediastinal cavity. This could be important in patients with hypereosinophilia, since we showed that hypereosinophilic mice have more eosinophils in their mediastinum than do WT mice. Our findings suggest that ILC2s may direct eosinophils to infiltrate organs, not only from the blood but also from the neighboring serosal cavity where these cells reside locally.

Serosal fluid in the pericardium contains immune cells and can become a source of infiltrating leukocytes under certain insults such as exposure following cardiac surgery and myocardial infarction (Butts et al., 2017; Horckmans et al., 2018). We found that ILCs were present at a higher frequency in the pericardial fluid of patients with pericarditis, whereas healthy controls and patients with other types of cardiac diseases such as cardiomyopathy showed a much lower frequency of ILCs in the pericardial fluid. The number of patients

tested was limited; therefore, further clinical investigation will be needed. However, this result suggests that ILCs may also be involved in the pathogenesis of pericarditis in humans. It is unclear whether the increase in ILCs results from other underlying causes such as infection and whether ILCs directly induce human pericarditis, as shown in the IL-33-induced pericarditis mouse model.

Although many pericarditis case reports have been published, the etiology is still largely unknown. Contemporary treatments for pericarditis mostly aim to resolve symptoms by administrating anti-inflammatory agents such as nonsteroidal anti-inflammatory drugs (NSAIDs, especially indomethacine), colchicine, and corticosteroids (Imazio et al., 2013, 2015). A phase III clinical trial (ClinicalTrials.gov: NCT03737110) is assessing the IL-1 blocker in patients with recurrent pericarditis. Another treatment option for severe cases is a pericardiocentesis or pericardiectomy to remove the inflamed pericardium. These symptomatic therapies, however, do not address a specific cause of pericarditis. One of the problems in developing new targeted therapies is a lack of classification on subtypes of pericarditis. There are several case reports of eosinophilic pericarditis in humans (Li et al., 2002; Spiegel et al., 2004; Herry et al., 1997; AbdullGaffar and Almulla, 2015; Van den Bosch et al., 1986). In this study, using the IL-33-induced eosinophilic pericarditis mouse model, we identified cardiac ILC2s playing a critical role in the pathogenesis of eosinophilic pericarditis. We also showed limited human data that suggest an increased number of ILCs in the pericardial fluid of pericarditis patients. These findings augment our understanding of how ILC2s contribute to cardiac inflammation and provide insights into targeted therapy for eosinophilic pericarditis. In a setting where there is no specific way to target ILC2s, it may be helpful to alleviate eosinophilic pericarditis by blocking the IL-33-ST2-ILC2s axis.

Our findings suggest a pathogenic role for ILCs in cardiac inflammation. ILCs play a critical role in the development of pericarditis induced by IL-33, as their presence and activation are essential components to inducing pericarditis. Our study provides insights into the role of cardiac ILCs in inflammation that can be helpful to developing therapeutic targets for pericarditis.

STAR★METHODS

LEAD CONTACT AND MATERIALS AVAILABILITY

This study did not generate new unique reagents. Further information and requests for resources and reagents should be directed to and will be fulfilled by the Lead Contact, Daniela Čiháková (cihakova@jhmi.edu).

EXPERIMENTAL MODEL AND SUBJECT DETAILS

Human samples—Human pericardial fluid samples were obtained from patients with pericarditis, ARVC, IHD or valve disease. Samples were collected while these patients underwent coronary artery bypass grafting, valve replacement surgery or pericardiocentesis at the Institute for Clinical and Experimental Medicine (IKEM) in Czech Republic. Informed consent was obtained from subjects and the study protocol was approved by the IKEM Ethics Committee (G-18-60). Control pericardial fluid specimens were obtained from

rapid autopsy of patients who had no cardiovascular diseases at the Johns Hopkins University. Informed consent was obtained from subjects and the study protocol was approved by the Committee for the Protection of Human Subjects (IRB NA_00036610, PI: Jody Hooper). Sex of human sample donors is indicated below: Controls, 1 male and 2 females; ARVC, 1 male and 2 females; IHD, 11 males and 4 females; Valve disease, 2 males and 2 females; Pericarditis, 1 male and 1 female. Pericardial fluid cells were isolated by centrifugation, resuspended in fetal bovine serum (FBS) supplemented with 10% DMSO, and stored in a liquid nitrogen tank. Frozen samples were shipped on dry ice. Patients' information of all samples was processed with random non-linked code labeling in a database at the time of preservation. For each sample, a separate random non-linked code was assigned for the analysis process.

Animals—Wild-type BALB/cJ (JAX 651), *Rag2*$^{-/-}$ (JAX 8448), *Rag2*$^{-/-}\gamma c^{-/-}$ (JAX 14593), CD45.1/cByJ (JAX 6584), ΔdblGATA1 (JAX 5653) mice were obtained from the Jackson Laboratory (Bar Harbor, ME). ST2$^{-/-}$, IL-13$^{-/-}$ and IL-33$^{cit/+}$ mice were kindly provided by Andrew N.J. McKenzie (Medical Research Council, Cambridge, UK). IL-33$^{cit/cit}$ mice were used as IL-33$^{-/-}$ mice. IL-5Tg mice were kindly provided by James Lee (Mayo Clinic, Scottsdale, AZ). Mice used were 6 to 12-week-old male mice on the BALB/c background unless otherwise mentioned in the figure legends. Mice were maintained at the Johns Hopkins University School of Medicine specific pathogen-free animal facility. Experiments were performed with age-matched mice in accordance with the guidelines set forth in the Guide for the Care and Use of Laboratory Animals. All methods and protocols were approved by the Animal Care and Use Committee of Johns Hopkins University.

Isolation of primary adult mouse cardiac fibroblasts—Hearts were isolated from 6-12-week-old WT BALB/c mice pretreated *i.p.* with PBS with 50U/ml Heparin. Hearts were cannulated through aorta and perfused for 3 min at 37°C with calcium-free perfusion buffer (7.03 g/L NaCl, 1.1 g/L KCl, 0.082 g/L KH_2PO_4, 0.085 g/L Na_2HPO_4, 0.144 g/L $MgSO_4$, 2.38 g/L HEPES, 0.39 g/L $NaHCO_3$, 1 g/L glucose, 3.74 g/L Taurine, 1 g/L 2,3-Butanedione monoxime; all Sigma-Aldrich) and for 8 min with the addition of Collagenase II (Worthington Biochemical Corporation) and Protease XIV (Sigma-Aldrich) and 0.03M CaCl2. The heart was cut into pieces and digested by gentle pipetting for 3 min or until large pieces are fully digested. After filtering through a 100 μm strainer and washing with DMEM (GIBCO), cardiac fibroblasts in cell suspensions were separated from cardiac myocytes that precipitated rapidly and spontaneously. Cardiac fibroblasts were cultured at 37°C in DMEM with 20% FBS (GE Healthcare Life Siences), Non-essential amino-acids (Sigma Aldrich), Penicillin-Streptomycin, 2 mM L-Glutamine, and 25 mM HEPES (all Quality Biological). Nonadherent cells were washed off after 1 h. Culture media was changed every day for 5 days until cardiac fibroblasts are confluent. Cardiac fibroblasts were passaged twice before co-culture.

METHOD DETAILS

Induction of experimental pericarditis—Mice were injected with 1 μg of recombinant mouse IL-33 (BioLegend) in 100 μL PBS intraperitoneally on days 0, 2, 4, 6 and 8. On day 9 or 10, hearts were harvested for further analysis detailed below.

Assessment of pericarditis severity—Hearts were cut transversely, fixed in SafeFix (Thermo Fisher Scientific), embedded in paraffin, cut into 5 μm-thick sections and stained with H&E (Histoserv, MD). The severity of pericarditis was assessed by scoring infiltration of the area of pericardium around right ventricle (RV) on H&E-stained sections based on histopathology score from 0 to 4 using the following criteria for hematopoietic infiltrates: grade 0, no inflammation; grade 1, < 20% of RV is involved and/or mild inflammation; grade 2, 20%–50% of RV is involved and/or intermediate inflammation; grade 3, 50%–80% of RV is involved and/or severe inflammation; grade 4, >80% of RV is involved and/or severe inflammation with adjacent myocardial infiltrates. Scoring was performed by two blinded investigators and averaged.

Light microscopy—Images on H&E-stained and immunostained sections were acquired on the BX43 microscope (Olympus) with the DS-Fi3 camera (Nikon) using NIS-Elements D Software (v. 5.10.01, Nikon).

Tissue clearing with immunolabeling and light sheet microscopy—Hearts were perfused with PBS for 3 min followed by 4% paraformaldehyde in PBS for 3 min for fixation. After perfusion, hearts were removed from mice and the right ventricle was obtained and immersed in 4% paraformaldehyde in PBS for 2 h at 4°C to complete fixation. After washing with PBS, the sample was permeabilized, washed, penetrated, and blocked using Visikol HISTO reagents (Visikol) according to manufacturer's protocols. Primary and secondary antibody staining were performed using 10 μg/ml anti-mouse SiglecF (BD) and KLRG1 (ProSci) antibodies and 20 μg/ml anti-rat and anti-hamster IgG conjugated with fluorophores (Thermo Fisher Scientific), respectively, in Visikol HISTO antibody buffer (Visikol) according to manufacturer's protocols. After immunolabeling, tissue clearing process was conducted using Visikol HISTO-1 and −2 (Visikol) following manufacturer's instruction. Images of cleared tissue with immunolabeling were acquired using a light sheet microscope, Ultra Microscope II (LaVision Biotec). Processing of images was carried out with Imaris (Bitplane).

Immunofluorescence staining and confocal microscopy—Mouse heart was perfused with PBS for 3 min followed by 4% paraformaldehyde in PBS for 3 min for fixation. After perfusion, heart was removed from mice and immersed in 4% paraformaldehyde in PBS for 2 h at 4°C to complete fixation. After fixation, the heart was placed in 30% sucrose in PBS overnight or until tissue sinks at 4°C before embedding in OCT. Cryostat sectioning was performed to obtain heart sections in a 100 μm-thickness. Sections were washed in PBS, permeabilized in 0.5% Triton X-100 in PBS and blocked in 10% normal goat serum and 0.3% Triton X-100 in PBS. After blocking, sections were incubated with Rabbit anti-PDGFRα antibody (Abcam). Goat anti-Rabbit IgG conjugated with Alexa Fluor 555 (Thermo Fisher) was used as secondary antibody and DAPI was used

for counterstaining. Images were acquired using Zeiss LSM 700 microscope (Zeiss) at 20X and 40X magnification with the ZEN Black software (Zeiss). ImageJ/Fiji was used to process images.

Immunohistochemistry staining—Paraffin-embedded hearts were cut into 4-μm-thick sections. After deparaffinization, heat-induced antigen retrieval and blocking, sections were stained with 5 μg/ml Polyclonal Goat Anti-Mouse CCL11 antibody (R&D Systems) and Anti-Goat HRP-DAB Cell & Tissue Staining Kit (R&D Systems) and counter stained with Hematoxylin.

Echocardiography—Conscious mice were held in a supine position and M-mode or Doppler echocardiography was performed using Vevo 2100 with a MS400 or MS550D transducer (FUJIFILM VisualSonics, Ontario, Canada). In M-mode, the heart was imaged in the parasternal short axis view to measure parameters such as left ventricular internal dimension (LVID) and ejection fraction (EF). To measure the Myocardial Performance Index (MPI), tissue Doppler imaging of the mitral annulus was obtained. Cardiac time intervals, isovolumetric contraction time (IVCT), isovolumetric relaxation time (IVRT) and ejection time (ET), were measured and MPI was calculated based on these parameters (Gao et al., 2011).

High-dimensional mass cytometry (CyTOF)—Frozen cells were thawed at 37°C and washed with PBS twice. Single cell suspensions were stained with Cell-ID Cisplatin (Fluidigm), blocked with Fc Receptor Binding Inhibitor (Thermo Fisher), and stained with heavy metal-conjugated antibodies (Fluidigm) for surface staining. Cells were fixed and permeabilized with FoxP3 Transcription Factor Staining Buffer Set (Thermo Fisher) followed by intracellular staining with metal-conjugated antibodies (Fluidigm). Cells were fixed in methanol-free formaldehyde (Thermo Fisher) and kept in Cell-ID Intercalator-Ir solution (Fluidigm). Stained cells were shipped on ice to the CyTOF Facility at the University of Pennsylvania and acquired on Helios (Fluidigm). CyTOF data were normalized in the CyTOF software (Fluidigm) and analyzed using Cytobank (Cytobank Inc).

Flow cytometry and cell sorting—Hearts were perfused with PBS through ventricles, cut into small pieces and digested in gentleMACS C Tubes (Miltenyi Biotec) with 3000U Collagenase II and 300U DNase I (Worthington Biochemical Corporation) in HBSS for 30 min at 37°C. To generate single cell suspensions, hearts were mechanically dissociated using GentleMACS dissociator (Miltenyi Biotec) following manufacturer's protocols. Cells in the mediastinal cavity were harvested by lavage with PBS. Blood was collected in PBS with 100U/ml Heparin and overlaid on Histopaque-1119 (Sigma Aldrich) to remove red blood cells. Remaining red blood cells were lysed using ACK buffer (Quality Biological). Cells from heart samples were strained through a 40 μm filter, and cells from other organs were strained through a 70 μm filter. For intracellular cytokine staining, cells were stimulated with 50 ng/ml PMA, 750 ng/ml Ionomycin (Sigma-Aldrich), GolgiStop and GolgiPlug (BD Biosciences) for 4 h at 37°C before staining. Single cell suspensions were stained with LIVE/DEAD Fixable Aqua (Thermo Fisher Scientific). FcγRII/III was blocked with anti-mouse CD16/CD32 (eBioscience), and markers of interest were stained with flourochrome-

conjugated antibodies (BD, BioLegend and eBioscience). Lineage (Lin) used for identifying mouse ILC2s included CD3ε, TCRβ, CD19, B220, CD11b, CD11c, Gr-1, Ter119, FcεRIα and NKp46. To quantify absolute number of cells, viable cells were counted using CountBright Absolute Counting Beads (Thermo Fisher Scientific). Samples were acquired on BD LSR II or Fortessa (BD Biosciences) and data were analyzed using FlowJo V10 (Tree Star). For cardiac ILC2 sorting, after enzymatic and mechanical dissociation of hearts, single cell suspensions were obtained using Histopaque-1077 (Sigma-Aldrich) according to manufacturer's instructions. Collected mononuclear cells were stained and sorted on BD FACSAria II (BD Biosciences).

Isolation and *in vitro* expansion of cardiac ILC2—Cardiac ILC2s were isolated using FACSAria II (BD Biosciences) from the hearts of IL-33-treated mice and cultured at 37°C in RPMI 1640 (GIBCO) with 10% FBS (GE Healthcare Life Sciences), 1% Penicillin-Streptomycin, 2 mM L-Glutamine, 10 mM HEPES, 1 mM Sodium Pyruvate (all Quality Biological), 0.1 mM Non-essential amino acids (Sigma Aldrich), 0.05 mM 2-Mercaptoethanol (GIBCO). Cytokines, IL-2, IL-7 and IL-33, at a concentration of 25 ng/ml were added in media to expand ILC2s *in vitro.*

Cardiac injection of ILC2—CD45.2^{+} *Rag2*$^{-/-}$ $\gamma c^{-/-}$ mice were anesthetized with 3.5% isoflurane (Baxter) and tracheal intubation was performed immediately. While on intubation, mice were provided with oxygen with 2% isoflurane by mechanical ventilation system (Model 845, Harvard Apparatus). Pre-operational analgesics (0.05 mg/kg Buprenorphine, Reckitt Benckiser) and paralytics (1 mg/kg Succinylcholine, Henry Schein) were treated before operation. Thoracotomy was done to access the chest cavity and expose the ventricles of the heart. 5x10^{5} CD45.1^{+} cardiac ILC2s were injected into the myocardium on three ventricular locations using a 29G ½ insulin syringe (BD). Post-operational analgesics (0.05 mg/kg Buprenorphine) were administered during recovery.

***In vitro* co-culture of cardiac fibroblasts and ILC2—**ILC2s were FACS-sorted from the hearts of I L-33-treated mice and expanded *in vitro* as described above. 1x10^{5} ILC2s were placed on Transwell with 0.4 μm pore polyester membrane insert (Corning). Cardiac fibroblasts from second passage were co-cultured with ILC2s located on Transwell at 37° C in ILC2 culture media for 24 h. 25 ng/ml IL-2 and 25 ng/ml IL-7 were included in co-culture and 25 ng/ml IL-33 was added in certain conditions indicated. Cells and supernatants were harvested after co-culture and used for further analysis.

***In vivo* IL-5 neutralization—**To block IL-5 *in vivo*, mice were treated *i.p.* with 300 μg of anti-IL-5 monoclonal antibody (Clone: TRFK5, BioXCell) or isotype antibody (Clone: HRPN, BioXCell) every three days starting from a day before pericarditis induction.

Eosinophil isolation, labeling, and transfer to the mediastinal cavity or intravenously—Blood from donor IL-5Tg mice was collected in PBS with 100U/ml Heparin and overlaid on Histopaque-1119 (Sigma Aldrich) to remove red blood cells. Anti-CD90.2 and anti-CD45R(B220) microbeads (Miltenyi Biotec) were used to deplete lymphocytes and enrich eosinophils. Eosinophil purity (78%–95%) was determined by flow cytometry. For labeling, cells were stained with either CellTrace™ Violet (CTV) or

CellTrace™ Far Red (CTFR) according to manufacturer's instructions (Thermo Fisher). Recipient mice were anesthetized with 500 μL avertin or isoflurane and 1-8x10^6 cells were injected to the mediastinal cavity or by retro-orbital injection using a 29G ½ insulin syringe (BD).

Quantitative PCR—RNA was extracted in TRIzol (Invitrogen) and cDNA was synthesized using iScript cDNA Synthesis Kit (Bio-Rad). Quantitative PCR was performed using Power SYBR Green PCR Master Mix (Applied Biosystems) and executed on MyiQ2 thermal cycler (Bio-Rad) using iQ5 optical system software (Bio-Rad). Acquired data were analyzed by the $2^{-\Delta\Delta Ct}$ method (Livak and Schmittgen, 2001). Threshold cycles were normalized to the expression of *Gapdh* and then to controls. Primers for genes (*Ccl11*: 5′-GAATCACCAACAA CAGATGCAC-3′ and 5′-ATCCTGGACCCACTTCTTCTT-3′, *Ccl24*: 5′-TCTTAGGGCCCTTCTTGGTG-3′ and 5′- AATTCCAGAAAAC CGAGTGG-3′, *Il5*: 5′-CTCTGTTGACAAGCAATGAGACG-3′ and 5′-TCTTCAGTATGTCTAGCCCCTG-3′, *Il13*: 5′-CCTGGCTCTTG CTTGCCTT-3′ and 5′-GGTCTTGTGTGATGTTGCTCA-3′, *Gapdh*: 5′-TTGATGGCAACAATCTCCAC-3′ and 5′-CGTCCCGTAGACA AAATGGT-3′) were commercially synthesized (Integrated DNA Technologies).

ELISA—Supernatants from cardiac fibroblasts co-culture with ILC2s or sera from mice were stored at −80°C prior to ELISA. Eotaxin-1 was determined by quantitative sandwich ELISA using Mouse CCL11/Eotaxin Quantikine ELISA Kit (R&D Systems) according to manufacturer's protocols. For anti-myosin IgM ELISA, plates were coated with 0.5 μg/well myosin heavy chain α peptide MyHC$\alpha_{614\text{-}62g}$ (Ac-SLKLMATLFSTYASAD; Genscript) and Alkaline Phosphatase AffiniPure goat anti-mouse IgM, μ chain specific (Jackson ImmunoResearch) at a 1:4000 dilution was used to detect anti-myosin IgM in sera.

QUANTIFICATION AND STATISTICAL ANALYSIS

Statistical analysis—Two group comparisons were performed using Student's t test for normally distributed data. Multiple group comparisons were performed using one-way ANOVA followed by Tukey's post hoc test. Mann-Whitney U test or Kruskal-Wallis H test for two groups or multiple groups, respectively, was used for nonparametric data. Pearson correlation coefficient, r, was calculated using correlation analysis in Prism 6 (GraphPad Software Inc.). Statistical analysis was conducted in Prism 6. Statistically significant comparisons were represented by asterisks: *, $p < 0.05$; **, $p < 0.01$; ***, $p < 0.001$. Statistical analysis details are also described in the figure legends.

DATA AND CODE AVAILABILITY

This study did not generate datasets.

Supplementary Material

Refer to Web version on PubMed Central for supplementary material.

ACKNOWLEDGMENTS

The authors would like to extend their gratitude to Jobert G. Barin, Nicola L. Diny, Megan K. Wood, David Hughes, Hannah Kalinoski, and Paul Delgado for insightful discussions; Megan K. Wood and Jiyeon Lee for manuscript editing; Dr. Andrew N.J. McKenzie (Medical Research Council, Cambridge, UK) for the ST2$^{-/-}$, IL-13$^{-/-}$ and IL-33$^{cit/+}$ mice; Dr. James Lee (Mayo Clinic, Scottsdale, AZ, USA) for the IL-5Tg mice; Xiaoling Zhang (Johns Hopkins Ross Flow Cytometry Core) for cell sorting; Djahida Bedja and Nadan Wang for echocardiography; Kevin Brown (Fluidigm) for the CyTOF antibody panel design; Takuya Ohtani (Penn Institute for Immunology at the University of Pennsylvania) for operating CyTOF and acquiring samples; and the animal resources at Johns Hopkins University. This work was supported by grants from the National Institutes of Health/National Heart, Lung, and Blood Institute (R01HL118183 and R01HL136586), the American Heart Association AWRP Winter 2017 Grant-in-Aid (17GRNT33700274), the Johns Hopkins 2015 Catalyst Award, and the American Heart Association 2019 Transformational Project Award (19TPA34910007) to D.C.; the Matthew Vernon Poyner (MVP) Memorial Myocarditis Research Fund to D.C. and Nisha Gilotra; the American Heart Association Predoctoral Fellowship (16PRE31170040) to H.S.C.; the Myocarditis Foundation 2018 Rhett Lundy Memorial Research Fellowship to T.W.; the Johns Hopkins Autoimmune Disease Research Center O'Leary-Wilson Fellowship, the Johns Hopkins Bloomberg School of Public Health Richard J. and Margaret Conn Himelfarb Student Support fund, and the Katherine E. Welsh Fellowship to X.H.; the Myocarditis Foundation 2016 Research Fellowship to G.C.; and the American Heart Association Postdoctoral Fellowship (16POST31330012) and American Autoimmune-Related Diseases Association (AARDA) 2016 Young Investigator Award to W.B.-B.

REFERENCES

AbdullGaffar B, and Almulla A (2015). Eosinophilic pericardial effusion in hypereosinophilic syndrome with restrictive cardiomyopathy. Cytopathology 26, 388–389. [PubMed: 25302417]

Abston ED, Barin JG, Cihakova D, Bucek A, Coronado MJ, Brandt JE, Bedja D, Kim JB, Georgakopoulos D, Gabrielson KL, et al. (2012). IL-33 independently induces eosinophilic pericarditis and cardiac dilation: ST2 improves cardiac function. Circ. Heart Fail 5, 366–375. [PubMed: 22454393]

Blanchard C, Mingler MK, Vicario M, Abonia JP, Wu YY, Lu TX, Collins MH, Putnam PE, Wells SI, and Rothenberg ME (2007). IL-13 involvement in eosinophilic esophagitis: transcriptome analysis and reversibility with glucocorticoids. J. Allergy Clin. Immunol 120, 1292–1300. [PubMed: 18073124]

Borchers MT, Ansay T, DeSalle R, Daugherty BL, Shen H, Metzger M, Lee NA, and Lee JJ (2002). In vitro assessment of chemokine receptor-ligand interactions mediating mouse eosinophil migration. J. Leukoc. Biol 71, 1033–1041. [PubMed: 12050190]

Bracamonte-Baran W, Chen G, Hou X, Talor MV, Choi HS, Davogustto G, Taegtmeyer H, Sung J, Hackam DJ, Nauen D, and Čiháková D (2019). Non-cytotoxic Cardiac Innate Lymphoid Cells Are a Resident and Quiescent Type 2-Commited Population. Front. Immunol 10, 634. [PubMed: 30984196]

Butts B, Goeddel LA, George DJ, Steele C, Davies JE, Wei CC, Varagic J, George JF, Ferrario CM, Melby SJ, and Dell'Italia LJ (2017). Increased Inflammation in Pericardial Fluid Persists 48 Hours After Cardiac Surgery. Circulation 136, 2284–2286. [PubMed: 29203568]

Cayrol C, and Girard JP (2014). IL-33: an alarmin cytokinewith crucial roles in innate immunity, inflammation and allergy. Curr. Opin. Immunol 31, 31–37. [PubMed: 25278425]

Chen WY, Hong J, Gannon J, Kakkar R, and Lee RT (2015). Myocardial pressure overload induces systemic inflammation through endothelial cell IL-33. Proc. Natl. Acad. Sci. USA 112, 7249–7254. [PubMed: 25941360]

Chen G, Bracamonte-Baran W, Diny NL, Hou X, Talor MV, Fu K, Liu Y, Davogustto G, Vasquez H, Taegtmeyer H, et al. (2018). Sca-1^{+} cardiac fibroblasts promote development of heart failure. Eur. J. Immunol 48, 1522–1538. [PubMed: 29953616]

Coronado MJ, Bruno KA, Blauwet LA, Tschöpe C, Cunningham MW, Pankuweit S, van Linthout S, Jeon ES, McNamara DM, Krejčí J, et al. (2019). Elevated Sera sST2 Is Associated With Heart Failure in Men ≤ 50 Years Old With Myocarditis. J. Am. Heart Assoc 8, e008968. [PubMed: 30638108]

Demyanets S, Kaun C, Pentz R, Krychtiuk KA, Rauscher S, Pfaffenberger S, Zuckermann A, Aliabadi A, Gröger M, Maurer G, et al. (2013). Components of the interleukin-33/ST2 system are

differentially expressed and regulated in human cardiac cells and in cells of the cardiac vasculature. J. Mol. Cell. Cardiol 60, 16–26. [PubMed: 23567618]

Deniset JF, Belke D, Lee WY, Jorch SK, Deppermann C, Hassanabad AF, Turnbull JD, Teng G, Rozich I, Hudspeth K, et al. (2019). Gata6(+) Pericardial Cavity Macrophages Relocate to the Injured Heart and Prevent Cardiac Fibrosis. Immunity 51, 131–140.e5. [PubMed: 31315031]

Diny NL, Hou X, Barin JG, Chen G, Talor MV, Schaub J, Russell SD, Klingel K, Rose NR, and Čiháková D (2016). Macrophages and cardiac fibroblasts are the main producers of eotaxins and regulate eosinophil trafficking to the heart. Eur. J. Immunol 46, 2749–2760. [PubMed: 27621211]

Doherty TA, Baum R, Newbury RO, Yang T, Dohil R, Aquino M, Doshi A, Walford HH, Kurten RC, Broide DH, and Aceves S (2015). Group 2 innate lymphocytes (ILC2) are enriched in active eosinophilic esophagitis. J. Allergy Clin. Immunol 136, 792–794.e3. [PubMed: 26233928]

Drake LY, Iijima K, Bartemes K, and Kita H (2016). Group 2 Innate Lymphoid Cells Promote an Early Antibody Response to a Respiratory Antigen in Mice. J. Immunol 197, 1335–1342. [PubMed: 27421480]

Eberl G, Colonna M, Di Santo JP, and McKenzie AN (2015). Innate lymphoid cells. Innate lymphoid cells: a new paradigm in immunology. Science 348, aaa6566. [PubMed: 25999512]

Farne HA, Wilson A, Powell C, Bax L, and Milan SJ (2017). Anti-IL5 therapies for asthma. Cochrane Database Syst. Rev 9, CD010834. [PubMed: 28933516]

Friões F, Lourenço P, Laszczynska O, Almeida PB, Guimarães JT, Januzzi JL, Azevedo A, and Bettencourt P (2015). Prognostic value of sST2 added to BNP in acute heart failure with preserved or reduced ejection fraction. Clin. Res. Cardiol 104, 491–499. [PubMed: 25586507]

Fukuo Y, Nakatani T, Shinohara H, and Matsuda T (1988). The mouse pericardium: it allows passage of particulate matter from the pleural to the pericardial cavity. Anat. Rec 222, 1–5. [PubMed: 3189880]

Gao S, Ho D, Vatner DE, and Vatner SF (2011). Echocardiography in Mice. Curr. Protoc. Mouse Biol 1, 71–83. [PubMed: 21743841]

Gasteiger G, Fan X, Dikiy S, Lee SY, and Rudensky AY (2015). Tissue residency of innate lymphoid cells in lymphoid and nonlymphoid organs. Science 350, 981–985. [PubMed: 26472762]

Griesenauer B, and Paczesny S (2017). The ST2/IL-33 Axis in Immune Cells during Inflammatory Diseases. Front. Immunol 8, 475. [PubMed: 28484466]

Ha SA, Tsuji M, Suzuki K, Meek B, Yasuda N, Kaisho T, and Fagarasan S (2006). Regulation of B1 cell migration by signals through Toll-like receptors. J. Exp. Med 203, 2541–2550. [PubMed: 17060475]

Halim TY, Krauss RH, Sun AC, and Takei F (2012). Lung natural helper cells are a critical source of Th2 cell-type cytokines in protease allergen-induced airway inflammation. Immunity 36, 451–463. [PubMed: 22425247]

Herry I, Philippe B, Hennequin C, Danel C, Lejeunne C, and Meyer G (1997). Acute life-threatening toxocaral tamponade. Chest 112, 1692–1693. [PubMed: 9404776]

Horckmans M, Bianchini M, Santovito D, Megens RTA, Springael JY, Negri I, Vacca M, Di Eusanio M, Moschetta A, Weber C, et al. (2018). Pericardial Adipose Tissue Regulates Granulopoiesis, Fibrosis, and Cardiac Function After Myocardial Infarction. Circulation 137, 948–960. [PubMed: 29167227]

Imai Y, Yasuda K, Sakaguchi Y, Haneda T, Mizutani H, Yoshimoto T, Nakanishi K, and Yamanishi K (2013). Skin-specific expression of IL-33 activates group 2 innate lymphoid cells and elicits atopic dermatitis-like inflammation in mice. Proc. Natl. Acad. Sci. USA 110, 13921–13926. [PubMed: 23918359]

Imazio M, Brucato A, Cemin R, Ferrua S, Maggiolini S, Beqaraj F, Demarie D, Forno D, Ferro S, Maestroni S, et al.; ICAP Investigators (2013). A randomized trial of colchicine for acute pericarditis. N. Engl. J. Med 369, 1522–1528. [PubMed: 23992557]

Imazio M, Gaita F, and LeWinter M (2015). Evaluation and Treatment of Pericarditis: A Systematic Review. JAMA 314, 1498–1506. [PubMed: 26461998]

Judd LM, Heine RG, Menheniott TR, Buzzelli J, O'Brien-Simpson N, Pavlic D, O'Connor L, Al Gazali K, Hamilton O, Scurr M, et al. (2016). Elevated IL-33 expression is associated with pediatric eosinophilic esophagitis, and exogenous IL-33 promotes eosinophilic esophagitis

development in mice. Am. J. Physiol. Gastrointest. Liver Physiol 310, G13–G25. [PubMed: 26514775]

Kim BS, and Artis D (2015). Group 2 innate lymphoid cells in health and disease. Cold Spring Harb. Perspect. Biol 7, a016337. [PubMed: 25573713]

Kim BS, Siracusa MC, Saenz SA, Noti M, Monticelli LA, Sonnenberg GF, Hepworth MR, Van Voorhees AS, Comeau MR, and Artis D (2013). TSLP elicits IL-33-independent innate lymphoid cell responses to promote skin inflammation. Sci. Transl. Med 5, 170ra16.

Kim HY, Chang YJ, Subramanian S, Lee HH, Albacker LA, Matangkasombut P, Savage PB, Mckenzie AN, Smith DE, Rottman JB, et al. (2012). Innate lymphoid cells responding to IL-33 mediate airway hyperreactivity independently of adaptive immunity. J. Allergy Clin. Immunol 129, 216–227.e1-e6. [PubMed: 22119406]

Klose CS, and Artis D (2016). Innate lymphoid cells as regulators of immunity, inflammation and tissue homeostasis. Nat. Immunol 17, 765–774. [PubMed: 27328006]

Küchler AM, Pollheimer J, Balogh J, Sponheim J, Manley L, Sorensen DR, De Angelis PM, Scott H, and Haraldsen G (2008). Nuclear interleukin-33 is generally expressed in resting endothelium but rapidly lost upon angiogenic or proinflammatory activation. Am. J. Pathol 173, 1229–1242. [PubMed: 18787100]

Lee NA, McGarry MP, Larson KA, Horton MA, Kristensen AB, and Lee JJ (1997). Expression of IL-5 in thymocytes/T cells leads to the development of a massive eosinophilia, extramedullary eosinophilopoiesis, and unique histopathologies. J. Immunol 158, 1332–1344. [PubMed: 9013977]

Li L, Xia Y, Nguyen A, Lai YH, Feng L, Mosmann TR, and Lo D (1999). Effects of Th2 cytokines on chemokine expression in the lung: IL-13 potently induces eotaxin expression by airway epithelial cells. J. Immunol 162, 2477–2487. [PubMed: 10072486]

Li Q, Gupta D, Schroth G, Loghin C, Letsou GV, and Buja LM (2002). Images in cardiovascular medicine. Eosinophilic pericarditis and myocarditis. Circulation 105, 3066. [PubMed: 12082004]

Lindman BR, Breyley JG, Schilling JD, Vatterott AM, Zajarias A, Maniar HS, Damiano RJ Jr., Moon MR, Lawton JS, Gage BF, et al. (2015). Prognostic utility of novel biomarkers of cardiovascular stress in patients with aortic stenosis undergoing valve replacement. Heart 101, 1382–1388. [PubMed: 26037104]

Livak KJ, and Schmittgen TD (2001). Analysis of relative gene expression data using real-time quantitative PCR and the 2(-Delta Delta C(T)) Method. Methods 25, 402–408. [PubMed: 11846609]

Matsukura S, Stellato C, Georas SN, Casolaro V, Plitt JR, Miura K, Kurosawa S, Schindler U, and Schleimer RP (2001). Interleukin-13 upregulates eotaxin expression in airway epithelial cells by a STAT6-dependent mechanism. Am. J. Respir. Cell Mol. Biol 24, 755–761. [PubMed: 11415942]

McCarthy CP, and Januzzi JL Jr. (2018). Soluble ST2 in Heart Failure. Heart Fail. Clin 14, 41–48. [PubMed: 29153199]

McKenzie GJ, Emson CL, Bell SE, Anderson S, Fallon P, Zurawski G, Murray R, Grencis R, and McKenzie AN (1998). Impaired development of Th2 cells in IL-13-deficient mice. Immunity 9, 423–432. [PubMed: 9768762]

Molofsky AB, Savage AK, and Locksley RM (2015). Interleukin-33 in Tissue Homeostasis, Injury, and Inflammation. Immunity 42, 1005–1019. [PubMed: 26084021]

Moore PE, Church TL, Chism DD, Panettieri RA Jr., and Shore SA (2002). IL-13 and IL-4 cause eotaxin release in human airway smooth muscle cells: a role for ERK. Am. J. Physiol. Lung Cell. Mol. Physiol 282, L847–L853. [PubMed: 11880312]

Moro K, Yamada T, Tanabe M, Takeuchi T, Ikawa T, Kawamoto H, Furusawa J, Ohtani M, Fujii H, and Koyasu S (2010). Innate production of T(H)2 cytokines by adipose tissue-associated c-Kit(+)Sca-1(+) lymphoid cells. Nature 463, 540–544. [PubMed: 20023630]

Moro K, Kabata H, Tanabe M, Koga S, Takeno N, Mochizuki M, Fukunaga K, Asano K, Betsuyaku T, and Koyasu S (2016). Interferon and IL-27 antagonize the function of group 2 innate lymphoid cells and type 2 innate immune responses. Nat. Immunol 17, 76–86. [PubMed: 26595888]

Moussion C, Ortega N, and Girard JP (2008). The IL-1-like cytokine IL-33 is constitutively expressed in the nucleus of endothelial cells and epithelial cells in vivo: a novel ‘alarmin’? PLoS One 3, e3331. [PubMed: 18836528]

Neill DR, Wong SH, Bellosi A, Flynn RJ, Daly M, Langford TK, Bucks C, Kane CM, Fallon PG, Pannell R, et al. (2010). Nuocytes represent a new innate effector leukocyte that mediates type-2 immunity. Nature 464, 1367–1370. [PubMed: 20200518]

Nussbaum JC, Van Dyken SJ, von Moltke J, Cheng LE, Mohapatra A, Molofsky AB, Thornton EE, Krummel MF, Chawla A, Liang HE, and Locksley RM (2013). Type 2 innate lymphoid cells control eosinophil homeostasis. Nature 502, 245–248. [PubMed: 24037376]

Pichery M, Mirey E, Mercier P, Lefrancais E, Dujardin A, Ortega N, and Girard JP (2012). Endogenous IL-33 is highly expressed in mouse epithelial barrier tissues, lymphoid organs, brain, embryos, and inflamed tissues: in situ analysis using a novel Il-33-LacZ gene trap reporter strain. J. Immunol 188, 3488–3495. [PubMed: 22371395]

Price AE, Liang HE, Sullivan BM, Reinhardt RL, Eisley CJ, Erle DJ, and Locksley RM (2010). Systemically dispersed innate IL-13-expressing cells in type 2 immunity. Proc. Natl. Acad. Sci. USA 107, 11489–11494. [PubMed: 20534524]

Rothenberg ME (1999). Eotaxin. An essential mediator of eosinophil trafficking into mucosal tissues. Am. J. Respir. Cell Mol. Biol 21, 291–295. [PubMed: 10460744]

Salimi M, Barlow JL, Saunders SP, Xue L, Gutowska-Owsiak D, Wang X, Huang LC, Johnson D, Scanlon ST, McKenzie AN, et al. (2013). A role for IL-25 and IL-33-driven type-2 innate lymphoid cells in atopic dermatitis. J. Exp. Med 210, 2939–2950. [PubMed: 24323357]

Sanada S, Hakuno D, Higgins LJ, Schreiter ER, McKenzie AN, and Lee RT (2007). IL-33 and ST2 comprise a critical biomechanically induced and cardioprotective signaling system. J. Clin. Invest 117, 1538–1549. [PubMed: 17492053]

Sánchez-Más J, Lax A, Asensio-López Mdel.C., Fernandez-Del Palacio MJ, Caballero L, Santarelli G, Januzzi JL, and Pascual-Figal DA (2014). Modulation of IL-33/ST2 system in postinfarction heart failure: correlation with cardiac remodelling markers. Eur. J. Clin. Invest. 44, 643–651. [PubMed: 24837094]

Schmitz J, Owyang A, Oldham E, Song Y, Murphy E, McClanahan TK, Zurawski G, Moshrefi M, Qin J, Li X, et al. (2005). IL-33, an interleukin-1-like cytokine that signals via the IL-1 receptor-related protein ST2 and induces T helper type 2-associated cytokines. Immunity 23, 479–490. [PubMed: 16286016]

Schneider CA, Rasband WS, and Eliceiri KW (2012). NIH Image to ImageJ: 25 years of image analysis. Nat. Methods 9, 671–675. [PubMed: 22930834]

Seki K, Sanada S, Kudinova AY, Steinhauser ML, Handa V, Gannon J, and Lee RT (2009). Interleukin-33 prevents apoptosis and improves survival after experimental myocardial infarction through ST2 signaling. Circ. Heart Fail 2, 684–691. [PubMed: 19919994]

Shimotakahara A, Kuebler JF, Vieten G, Metzelder ML, Petersen C, and Ure BM (2007). Pleural macrophages are the dominant cell population in the thoracic cavity with an inflammatory cytokine profile similar to peritoneal macrophages. Pediatr. Surg. Int 23, 447–451. [PubMed: 17205294]

Spiegel R, Miron D, Fink D, Gavriel H, and Horovitz Y (2004). Eosinophilic pericarditis: a rare complication of idiopathic hypereosinophilic syndrome in a child. Pediatr. Cardiol 25, 690–692. [PubMed: 14743307]

Spits H, and Cupedo T (2012). Innate lymphoid cells: emerging insights in development, lineage relationships, and function. Annu. Rev. Immunol 30, 647–675. [PubMed: 22224763]

Spits H, Artis D, Colonna M, Diefenbach A, Di Santo JP, Eberl G, Koyasu S, Locksley RM, McKenzie AN, Mebius RE, et al. (2013). Innate lymphoid cells–a proposal for uniform nomenclature. Nat. Rev. Immunol 13, 145–149. [PubMed: 23348417]

Takahashi K, Imaeda H, Fujimoto T, Ban H, Bamba S, Tsujikawa T, Sasaki M, Fujiyama Y, and Andoh A (2013). Regulation of eotaxin-3/CC chemokine ligand 26 expression byThelpertype 2 cytokines in human colonic myofibroblasts. Clin. Exp. Immunol 173, 323–331. [PubMed: 23607908]

Townsend MJ, Fallon PG, Matthews DJ, Jolin HE, and McKenzie AN (2000). T1/ST2-deficient mice demonstrate the importance of T1/ST2 in developing primary T helper cell type 2 responses. J. Exp. Med 191, 1069–1076. [PubMed: 10727469]

Travers J, Rochman M, Caldwell JM, Besse JA, Miracle CE, and Rothenberg ME (2017). IL-33 is induced in undifferentiated, non-dividing esophageal epithelial cells in eosinophilic esophagitis. Sci. Rep 7, 17563. [PubMed: 29242581]

Van den Bosch JM, Wagenaar SS, and Westermann CJ (1986). Asthma, eosinophilic pleuropneumonia, and pericarditis without vasculitis. Thorax 41, 571–572. [PubMed: 3787538]

von Moltke J, and Locksley RM (2014). I-L-C-2 it: type 2 immunity and group 2 innate lymphoid cells in homeostasis. Curr. Opin. Immunol 31,58–65. [PubMed: 25458996]

Walker JA, Barlow JL, and McKenzie AN (2013). Innate lymphoid cells–how did we miss them? Nat. Rev. Immunol 13, 75–87. [PubMed: 23292121]

Wang J, and Kubes P (2016). A Reservoir of Mature Cavity Macrophages that Can Rapidly Invade Visceral Organs to Affect Tissue Repair. Cell 765, 668–678.

Weber GF, Chousterman BG, Hilgendorf I, Robbins CS, Theurl I, Gerhardt LM, Iwamoto Y, Quach TD, Ali M, Chen JW, et al. (2014). Pleural innate response activator B cells protect against pneumonia via a GM-CSF-IgM axis. J. Exp. Med 211, 1243–1256. [PubMed: 24821911]

Wong SH, Walker JA, Jolin HE, Drynan LF, Hams E, Camelo A, Barlow JL, Neill DR, Panova V, Koch U, et al. (2012).Transcription factor RORa is critical for nuocyte development. Nat. Immunol 13, 229–236. [PubMed: 22267218]

Zuo L, Fulkerson PC, Finkelman FD, Mingler M, Fischetti CA, Blanchard C, and Rothenberg ME (2010). IL-13 induces esophageal remodeling and gene expression by an eosinophil-independent, IL-13R alpha 2-inhibited pathway. J. Immunol 185, 660–669. [PubMed: 20543112]

Highlights

- ILCs are required for the development of IL-33-induced eosinophilic pericarditis
- ILC2s facilitate eotaxin expression in cardiac fibroblasts
- Eosinophils in the mediastinum can migrate to the heart during pericarditis
- ILCs are more frequently present in the pericardial fluid of pericarditis patients

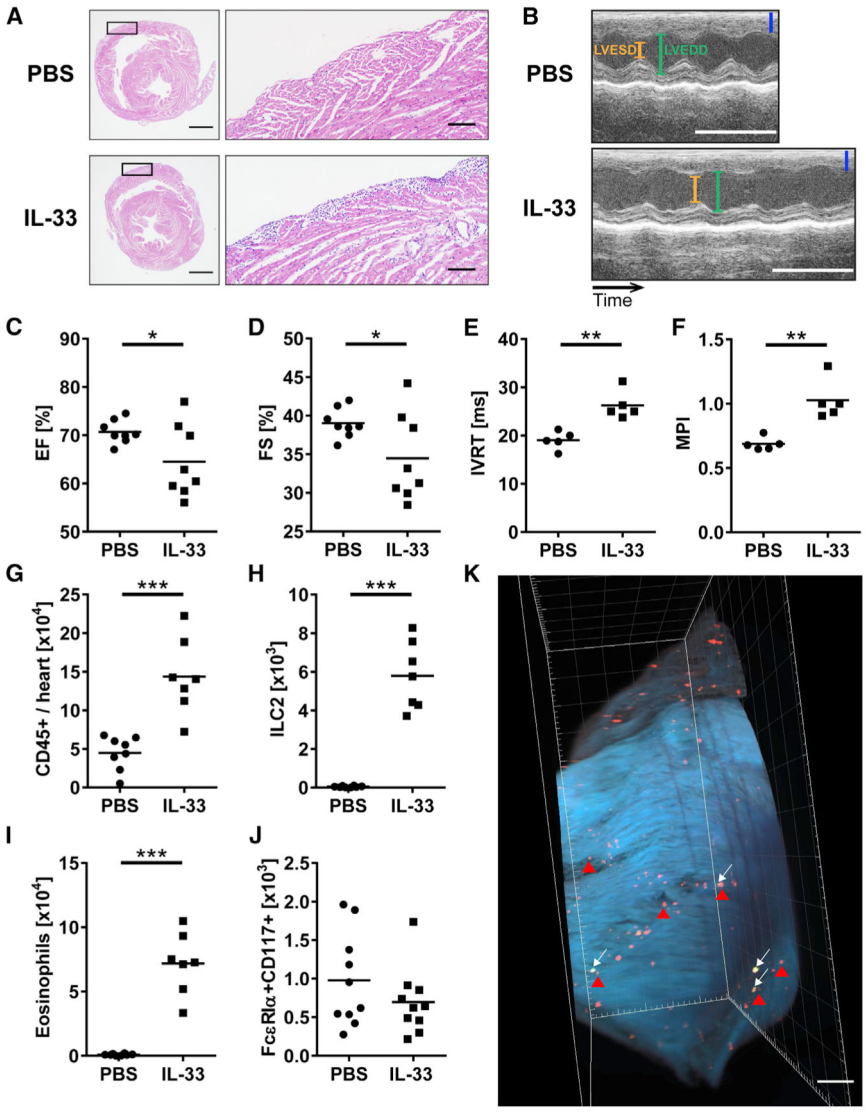

Figure 1. ILC2s Increases in the Heart, and Cardiac Function Is Changed following IL-33 Treatment

(A) Representative images of H&E-stained heart sections of the median mice treated with either PBS or IL-33. Areas marked by rectangles are shown as enlarged images in the right panels. Bars: 1 mm (left) and 100 μm (right).

(B) Representative M-mode pictures of animals treated with PBS or IL-33. Bars: blue, 1 mm; white, 0.1 s. LVESD, left ventricular end-systolic diameter; LVEDD, left ventricular end-diastolic diameter.

(C and D) Ejection fraction (EF) (C) and fractional shortening (FS) (D) of WT mice treated with PBS or IL-33.

(E and F) Isovolumetric relaxation time (IVRT) (E) and myocardial performance indexes (MPI) (F) of the heart from mice treated with PBS or IL-33 were assessed by Doppler echocardiography on day 9 post-PBS or IL-33 treatment.

(G) Total number of heart-infiltrating $CD45^+$ leukocytes was determined by flow cytometry.

(H–J) Number of (H) ILC2s, (I) eosinophils, and (J) mast cells in the hearts. Absolute cell counts per heart were calculated using counting beads for flow cytometry (see Method Details).

(K) Image of the right ventricle of the heart from *Rag2*$^{-/-}$ mice treated with IL-33. Green and red dots represent KLRG1^{+} ILC2s (white arrows) and SiglecF^{+} eosinophils (red arrowheads), respectively. Scale bar: 500 μm. Data are representative of three independent experiments.

Data are displayed as the means. Unpaired t test (C–J) was used for statistical analysis. *$p < 0.05$; **$p < 0.01$; ***$p < 0.001$.

See also Figures S1 and S2 and Video S1.

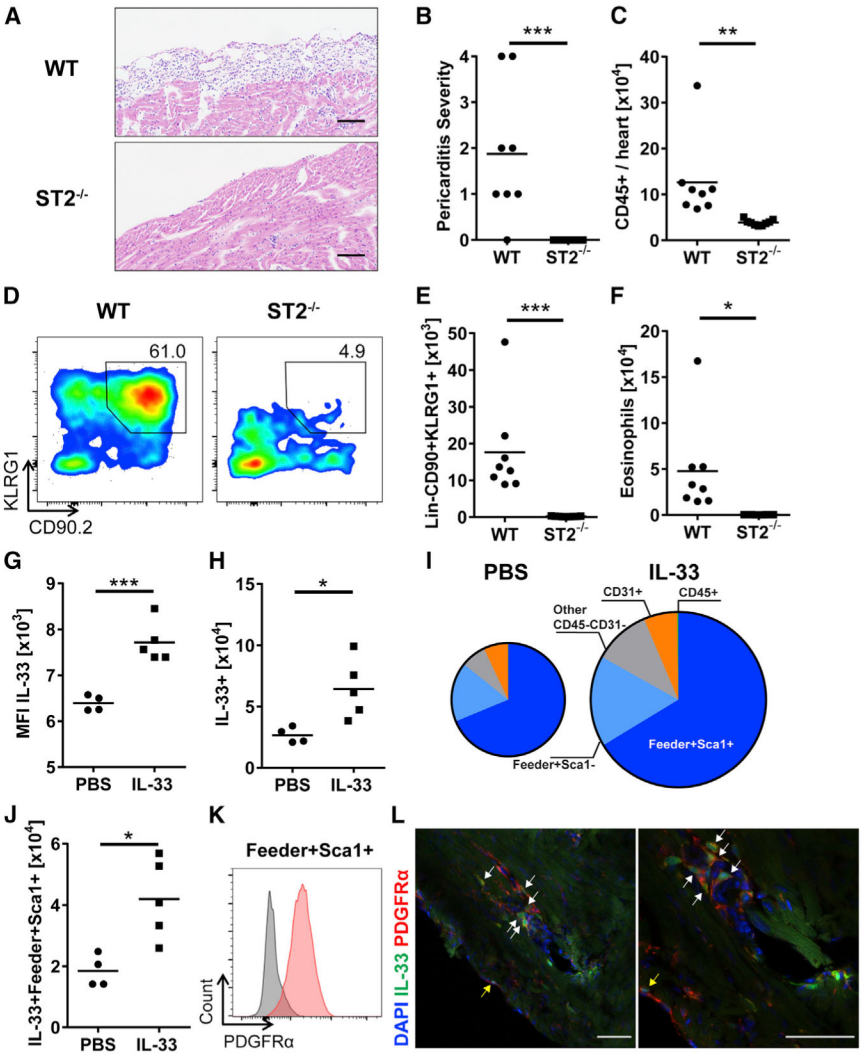

Figure 2. IL-33-ST2 Axis Is Critical for the Development of Pericarditis

(A) Representative images of H&E-stained heart sections of WT and ST2$^{-/-}$ mice. Bars: 100 μm.

(B) Severity of pericarditis was scored on H&E-stained heart sections.

(C) Number of heart-infiltrating CD45^{+} leukocytes was determined by flow cytometry.

(D) Representative flow cytometry plots of CD45^{+}Lin^{-} cells. Gates show the frequency of CD90^{+}KLRG1^{+} ILCs in the heart of WT and ST2$^{-/-}$ mice.

(E and F) Number of (E) Lin^{-}CD90^{+}KLRG1^{+} ILCs and (F) eosinophils in the hearts.

(G) Mean fluorescence intensity (MFI) of IL-33 expression in cardiac viable cells.

(H) Number of IL-33-expressing cells in the hearts.

(I) Mean frequency of different IL-33-expressing populations. The mean was quantified using values in a PBS-treated group (n = 4) and an IL-33-treated group (n = 5). Areas of the pie charts are proportional to total IL-33^{+} cells in the heart.

(J) Total number of IL-33^{+}Sca1^{+} cardiac fibroblasts.

(K) PDGFRα expression by Sca1^{+} cardiac fibroblasts.

(L) Immunofluorescence imaging shows IL-33-expressing PDGFRα$^+$ cardiac fibroblasts near the pericardium (white arrows) and in the pericardium (yellow arrows). Blue, green, and red color represent DAPI, IL-33, and PDGFRα, respectively. Bars: 50 μm.

Data are representative of two independent experiments and displayed as the mean. Mann-Whitney *U* test (B) or unpaired t test (C, E–H, and J) was used for statistical analysis. *p < 0.05; **p < 0.01; ***p < 0.001.

See also Figure S3.

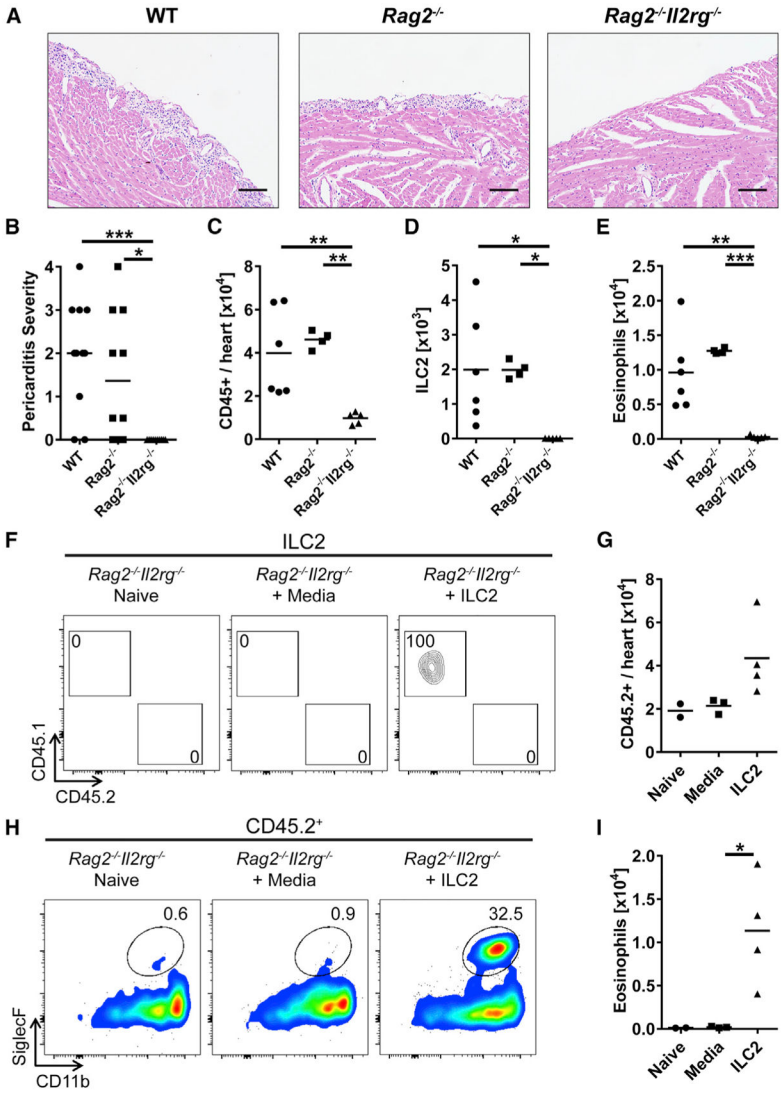

Figure 3. ILCs Are Required for the Development of Pericarditis, and ILC2s Are Sufficient to Induce Eosinophilic Infiltration to the Heart

(A) Representative images of H&E-stained heart sections of WT (left), *Rag2*$^{-/-}$ (center), and *Rag2*$^{-/-}$ *Il2rg*$^{-/-}$ (right) mice. Bars: 100 μm.

(B) Severity of pericarditis was scored on H&E-stained heart sections.

(C) Total number of heart-infiltrating CD45^{+} leukocytes was determined by flow cytometry.

(D and E) Number of (D) ILC2s and (E) eosinophils in the hearts.

(F) Representative flow cytometry plots of ILC2s found in the hearts of naive *Rag2*$^{-/-}$ *Il2rg*$^{-/-}$ mice and *Rag2*$^{-/-}$ *Il2rg*$^{-/-}$ mice injected with media or ILC2s followed by IL-33 treatment.

(G) Number of heart-infiltrating CD45.2^{+} leukocytes.

(H) Representative flow cytometry plots of CD45.2^{+} cells. Gates show the frequency of CD11b^{+}SiglecF^{+} eosinophils in the hearts of naive *Rag2*$^{-/-}$ *Il2rg*$^{-/-}$ mice and *Rag2*$^{-/-}$ *Il2rg*$^{-/-}$ mice injected with media or ILC2s followed by IL-33 treatment.

(I) Number of eosinophils in the hearts.

Both male and female mice were used in each group in (B). Data are representative of two independent experiments and displayed as the mean. Kruskal-Wallis H test (B) or one-way ANOVA followed by Tukey's post hoc test (C–E, G, and I) was used for statistical analysis. *$p < 0.05$; **$p < 0.01$; ***$p < 0.001$.

See also Figure S4.

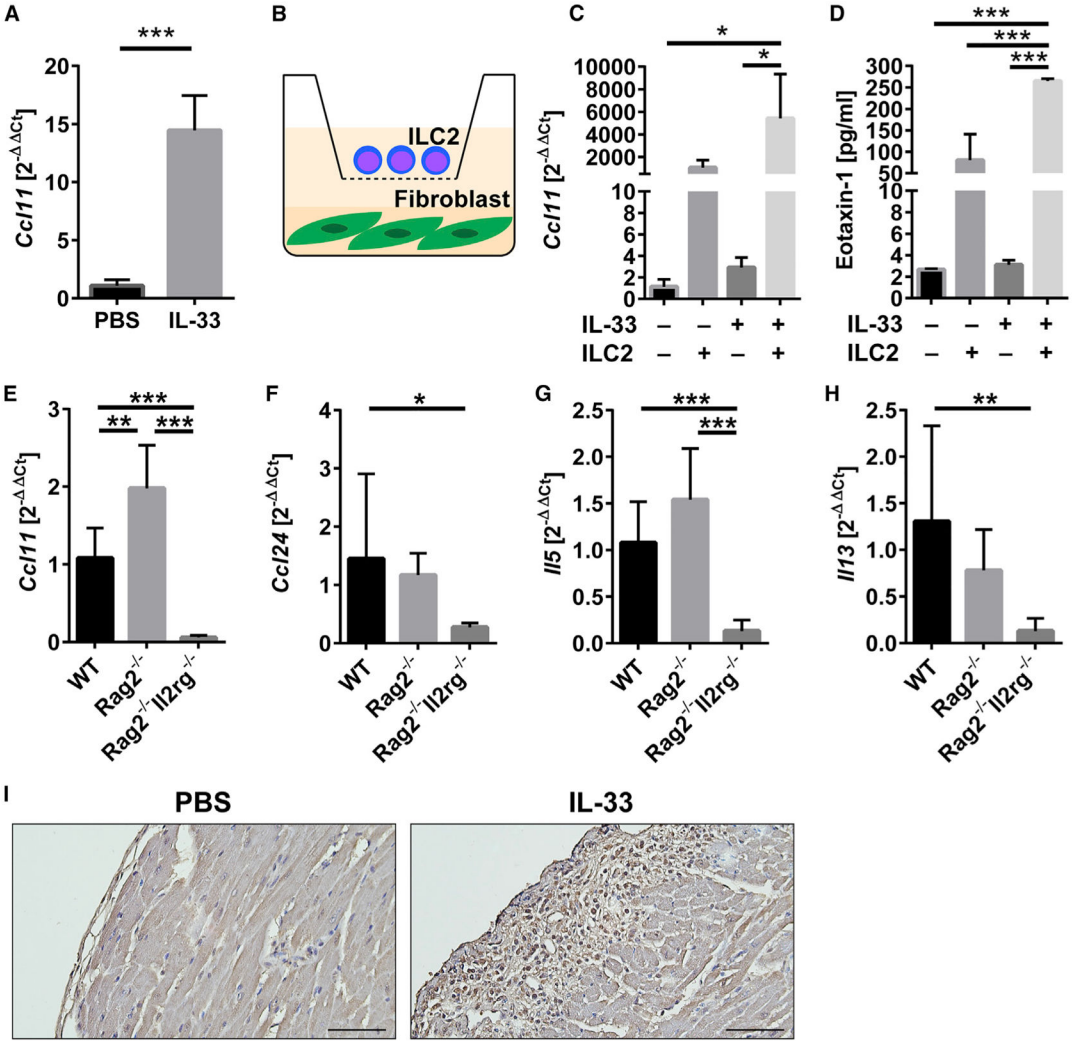

Figure4. Cardiac Fibroblasts Increase CCL11/Eotaxin-1 Expression and Production When Co-cultured with IL-33-Stimulated ILC2s, and the Expression of Eotaxins and Type 2 Cytokines Is Dependent on ILCs

(A) Expression of the *Ccl11* gene encoding eotaxin-1 in heart homogenates was analyzed by qPCR.

(B) Schematic description of cardiac fibroblasts co-culture with ILC2s separated by 0.4-μm transwell.

(C) Expression of *Ccl11* in cardiac fibroblasts was analyzed by qPCR.

(D) Eotaxin-1 concentrations in cell culture supernatants were measured by ELISA. IL-2 and IL-7 were included in culture media and IL-33 was added where indicated (C and D).

(E–H) Expression of genes in heart homogenates from WT, *Rag2*$^{-/-}$, and *Rag2*$^{-/-}$*Il2rg*$^{-/-}$ mice treated with IL-33 was analyzed by qPCR. *Ccl11* (E), *Ccl24* (F), *Il5* (G), and *Il13* (H).

(I) Immunohistochemistry staining for CCL11 of heart sections from WT mice treated with PBS or IL-33. Bars: 50 μm.

Data are representative of two independent experiments and displayed as the mean with SD. Unpaired t test (A) or one-way ANOVA followed by Tukey's post hoc test (C–H) was used for statistical analysis. *$p < 0.05$; **$p < 0.01$; ***$p < 0.001$.

See also Figure S5.

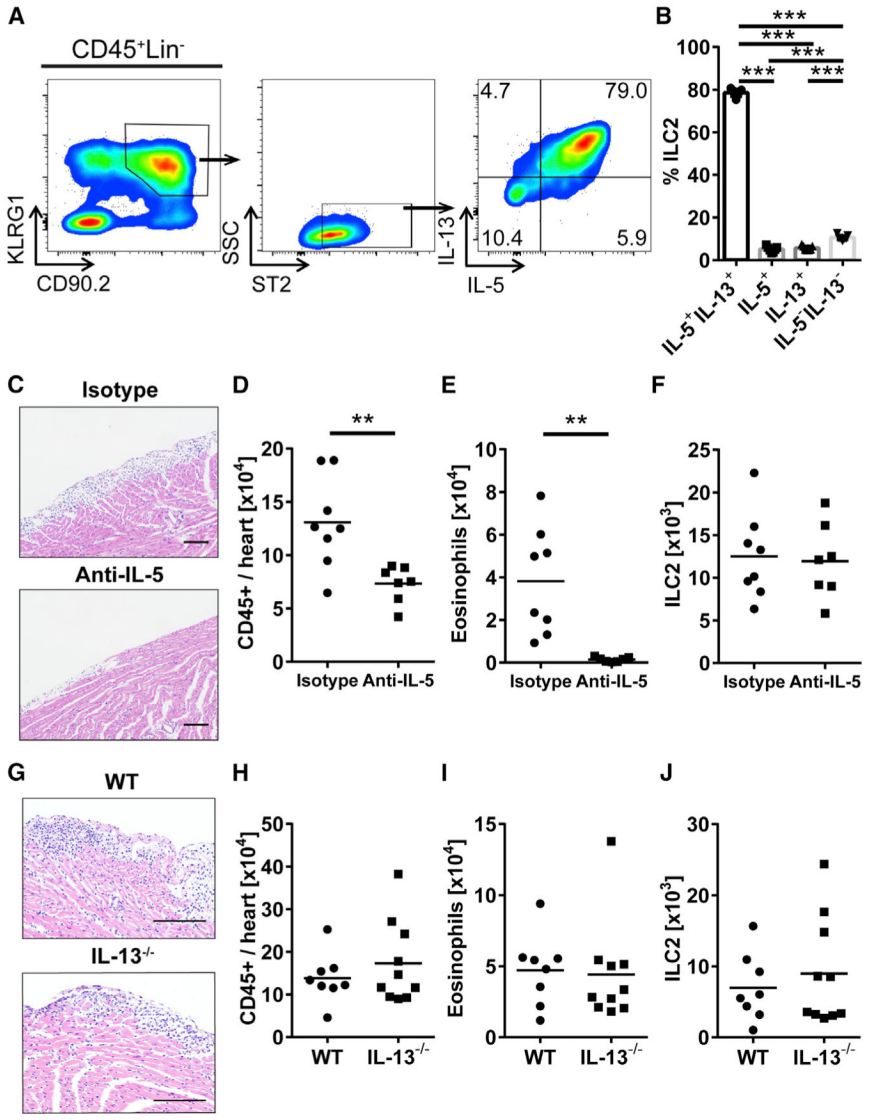

Figure 5. IL-5 Produced by ILC2s Play a Role during the Development of Pericarditis

(A) Representative flow cytometry plot of intracellular staining of IL-5 and IL-13 in cardiac ILC2s from IL-33-treated mice.

(B) Frequency of ILC2s producing IL-5 and/or IL-13 in the hearts of IL-33-treated mice.

(C) Representative images of H&E-stained heart sections of IL-33-treated mice with isotype or anti-IL-5 administration. Bars: 100 μm.

(D) Total number of heart-infiltrating $CD45^+$ leukocytes.

(E and F) Number of (E) eosinophils and (F) ILC2s in the hearts of IL-33-treated WT mice with isotype or anti-IL-5 administration.

(G) Representative images of H&E-stained heart sections of IL-33-treated WT and IL-$13^{-/-}$ mice. Bars: 100 μm.

(H) Total number of heart-infiltrating $CD45^+$ leukocytes.

(I and J) Number of (I) eosinophils and (J) ILC2s in the hearts of IL-33-treated WT and IL-$13^{-/-}$ mice. Data are representative of two independent experiments and displayed as the

mean. One-way ANOVA followed by Tukey's post hoc test (B) or unpaired t test (D–F and H–J) was used for statistical analysis. **$p < 0.01$; ***$p < 0.001$.

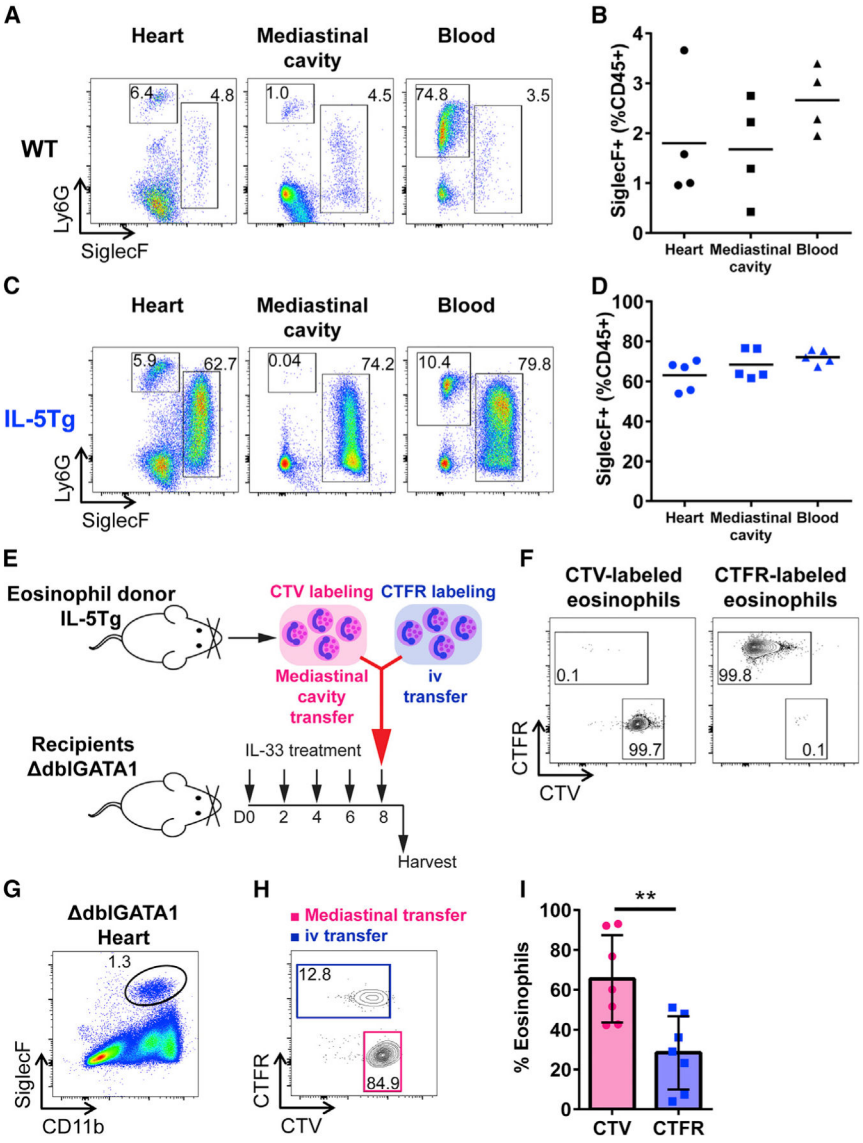

Figure 6. Eosinophils Reside in the Mediastinal Cavity from Which These Cells Can Traffic to the Heart

(A) Representative flow cytometry plot of $CD45^+CD11b^+$ cells. Gates show $CD11b^+SiglecF^+$ eosinophils and $CD11b^+Ly6G^+$ neutrophils in the heart, mediastinal cavity, and blood of WT naive mice.

(B) Frequency of eosinophils in the heart, mediastinal cavity, and blood of WT naive mice.

(C) Representative flow cytometry plot of $CD45^+CD11b^+$ cells. Gates show $CD11b^+SiglecF^+$ eosinophils and $CD11b^+Ly6G^+$ neutrophils in the heart, mediastinal cavity, and blood of IL-5Tg naive mice.

(D) Frequency of eosinophils in the heart, mediastinal cavity, and blood of IL-5Tg naive mice.

(E) Schematic description of eosinophil transfer to eosinophil-deficient ΔdblGATA1 mice.

(F) Flow cytometry plots of CTV- or CTFR-labeled eosinophils.

(G) Flow cytometry plot of $CD45^+$ cells in the heart. Gate shows $CD11b^+SiglecF^+$ eosinophils found in the heart of ΔdblGATA1 mice treated with IL-33 after eosinophil transfer in the mediastinal cavity and i.v.
(H) CTV- or CTFR-labeled $CD11b^+SiglecF^+$ eosinophils found in the heart of ΔdblGATA1 mice treated with IL-33 after eosinophil transfer.
(I) Frequency of CTV- or CTFR-labeled eosinophils found in the heart of ΔdblGATA1 mice treated with IL-33.
Concatenated samples (n = 7) are shown in (G) and (H). Both male and female mice were used in (G)–(I). Data are representative of two independent experiments and displayed as the mean (B and D) or the mean with SD (I). One-way ANOVA followed by Tukey's post hoc test (B and D) or unpaired t test (I) was used for statistical analysis. $^{**}p < 0.01$.
See also Figure S6.

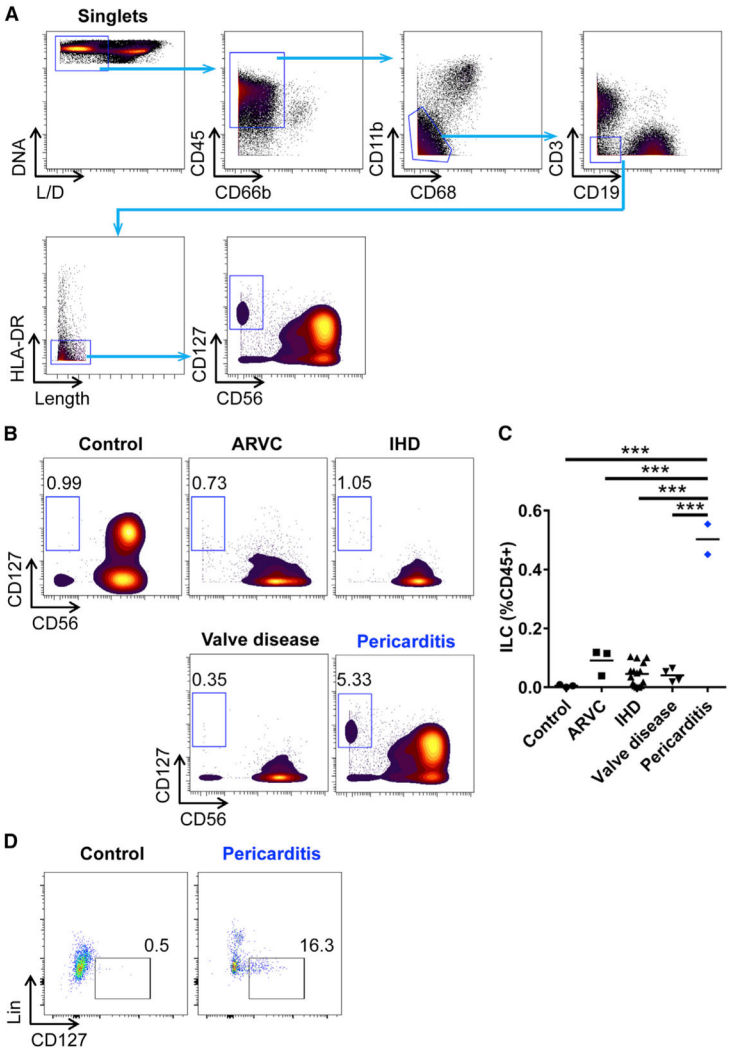

Figure 7. ILCs Are Increased in the Pericardial Fluid from Patients with Pericarditis

(A) Gating strategy of ILCs in human pericardial fluid samples by CyTOF. L/D, live/dead.

(B) Representative CyTOF plots showing ILCs in the pericardial fluid from controls and patients with cardiac diseases. ARVC, arrhythmogenic right ventricular cardiomyopathy; IHD, ischemic heart disease.

(C) Frequency of ILCs in the pericardial fluid.

(D) Flow cytometry plots showing $Lin^{-}CD127^{+}$ ILCs in the pericardial fluid from controls and patients with pericarditis. Plots show a $CD45^{+}CD11b^{-}CD3^{-}CD19^{-}CD56^{-}$ population. Lin included CD1a, CD11c, CD14, CD34, CD123, CD303a(BDCA2), TCRαβ, and FcεRIα.

Concatenated samples (control, n = 3; pericarditis, n = 2) are shown in (D). One-way ANOVA followed by Tukey's post hoc test (C) was used for statistical analysis. ***$p < 0.001$.

KEY RESOURCES TABLE

REAGENT or RESOURCE	SOURCE	IDENTIFIER
Antibodies		
Table S1	N/A	N/A
Biological Samples		
Pericardial fluid samples	Johns Hopkins University School of Medicine	https://www.hopkinsmedicine.org/som/
Pericardial fluid samples	Institute for Clinical and Experimental Medicine, Prague, Czech Republic	https://www.ikem.cz/en/
Chemicals, Peptides, and Recombinant Proteins		
Recombinant Mouse IL-33 (carrier-free)	BioLegend	Cat#580508
Collagenase, Type 2	Worthington	Cat#LS004177
Deoxyribonuclease I	Worthington	Cat#LS002139
Protease, Type XIV: Bacterial, From *Streptomyces griseus*	Sigma	Cat#P5147-5G
ACK Lysing Buffer	Quality Biological	Cat#118-156-721
Bovine Serum Albumin	Sigma	Cat#A3608-100G
0.5M EDTA, pH8.0	Corning	Cat#46-034-CI
PMA	Sigma	Cat#P1585
Ionomycin	Sigma	Cat#I9657
BD GolgiPlug	BD Biosciences	Cat#555029
BD GolgiStop	BD Biosciences	Cat#554724
LIVE/DEAD Fixable Aqua Dead Cell Stain Kit	Thermo Fisher	Cat#L34966
BV711 Streptavidin	BioLegend	Cat#405241
Streptavidin Alexa Fluor 350 Conjugate	Thermo Fisher	Cat#S11249
BD CytoFix Fixation Buffer	BD Biosciences	Cat#554655
Fixation/Permeabilization Solution Set	BD Biosciences	Cat#554714
eBioscience Foxp3/Transcription Factor Staining Buffer Set	Thermo Fisher	Cat#00-5523-00
CountBright Absolute Counting Beads	Thermo Fisher	Cat#C36950
SafeFix II All-Purpose Fixative	Fisher Scientific	Cat#23-042600
DMEM	GIBCO	Cat#11995-065
RPMI 1640	GIBCO	Cat#11875-093
Heat Inactivated Fetal Bovine Serum	Thermo Fisher	Cat#10082147
L-Glutamine	Corning	Cat#25-005-CI
Penicillin-Streptomycin	Sigma	Cat#P4333
Antibiotic-Antimycotic solution (100x)	Corning	Cat#30-004-CI
Sodium Pyruvate	Sigma	Cat#S8636
1M HEPES Buffer pH7.3	Quality Biological	Cat#118-089-721
MEM Non-essential Amino Acid solution (100x)	Sigma	Cat#M7145-100ML
2-Mercaptoethanol	GIBCO	Cat#21985-023
Recombinant Mouse IL-2 (carrier-free)	BioLegend	Cat#575404
Recombinant Mouse IL-7 (carrier-free)	BioLegend	Cat#577802
Heparin sodium salt from porcine intestinal mucosa	Sigma	Cat#H3393

REAGENT or RESOURCE	SOURCE	IDENTIFIER
Trypsin 2.5%	Quality Biological	Cat#118-086-721
Histopaque-1119	Sigma	Cat#11191-100ML
Histopaque-1077	Sigma	Cat#10771-100ML
CD90.2 MicroBeads, mouse	Miltenyi Biotec	Cat#130-049-101
CD45R (B220) MicroBeads, mouse	Miltenyi Biotec	Cat#130-049-501
TRIzol Reagent	Thermo Fisher	Cat#15596026
iScript cDNA Synthesis Kit	Bio-Rad	Cat#1708891
Power SYBR Green PCR Master Mix	Thermo Fisher	Cat#4367659
Normal Goat Serum Blocking Solution	Vector Laboratories	Cat#S-1000-20
Prolong Glass Antifade Mountant	Thermo Fisher	Cat#P36980
Visikol HISTO Starter Kit	VISIKOL	Cat#HSK-1
Forane Liquid for inhalation 100ml	Baxter	Cat#1001936040
Buprenorphine(1mg/ml)	ZooPharm	Cat#BZ8069317
Succinylcholine (20mg/ml)	Hospira, Inc.	Cat#00409662902
CellTrace Violet Cell Proliferation Kit	Thermo Fisher	Cat#C34557
CellTrace Far Red Cell Proliferation Kit	Thermo Fisher	Cat#C34564
MyHC$\alpha_{614\text{-}629}$ (Ac-SLKLMATLFSTYASAD)	GenScript	N/A
Trilogy	Cell Marque	Cat#920P-04
TBS with Tween (TBST), 20X Solution	Thermo Fisher	Cat#J75500-K2
Dual Endogenous Enzyme Block	Dako	Cat#S2003
Antibody Dilution Buffer	Ventana	Cat#ADB250
Richard-Allan Scientific Signature Series Hematoxylin 1	Thermo Fisher	Cat#7221
Richard-Allan Scientific Signature Series Clear-Rite 3	Thermo Fisher	Cat#6901
Shandon Bluing Reagent	Thermo Fisher	Cat#6769001
Optic Mount I Toluene	Mercedes Scientific	Cat#MER7722
Maxpar PBS	Fluidigm	Cat#201058
Cell-ID Intercalator-Ir	Fluidigm	Cat#201192B
Cell-ID Cisplatin	Fluidigm	Cat#201064
Maxpar Cell Staining Buffer	Fluidigm	Cat#201068
Maxpar Fix and Perm Buffer	Fluidigm	Cat#201067
16% Formaldehyde (w/v), Methanol-free	Thermo Fisher	Cat#28906
Critical Commercial Assays		
Mouse CCL11/Eotaxin-1 Quantikine ELISA Kit	R&D Systems	Cat#MME00
Anti-Goat HRP-DAB Cell & Tissue Staining Kit	R&D Systems	Cat#CTS008
Experimental Models: Organisms/Strains		
Mouse: WT: BALB/cJ	The Jackson Laboratory	Cat#000651
Mouse: CD45.1^{+}: CByJ.SJL(B6)-*Ptprc^{a}*/J	The Jackson Laboratory	Cat#006584
Mouse: *Rag2$^{-/-}$*: C.B6(Cg)-*Rag2$^{tm1.1Cgn}$*/J	The Jackson Laboratory	Cat#008448
Mouse: *Rag2$^{-/-}$ Il2rg$^{-/-}$*: C;129S4-*Rag2$^{tm1.1Flv}$ Il2rg$^{tm1.1Flv}$*/J	The Jackson Laboratory	Cat#014593
Mouse: ΔdblGATA1: C.129S1(B6)-*Gata1^{tm6Sho}*/J	The Jackson Laboratory	Cat#005653
Mouse: ST2$^{-/-}$ (BALB/c)	Townsend et al., 2000 (Dr. McKenzie)	N/A

REAGENT or RESOURCE	SOURCE	IDENTIFIER
Mouse: IL-13$^{-/-}$ (BALB/c)	McKenzie et al., 1998 (Dr. McKenzie)	N/A
Mouse: IL-33$^{cit/+}$ (BALB/c)	Wong et al., 2012 (Dr. McKenzie)	N/A
Mouse: IL-33$^{-/-}$: IL-33$^{cit/cit}$ (BALB/c)	This paper	N/A
Mouse: IL-5Tg (BALB/c)	Lee et al., 1997 (Dr. Lee)	N/A
Oligonucleotides		
Ccl11 forward primer: 5′-GAATCACC AACAACAGATGCAC-3′	This paper	N/A
Ccl11 reverse primer: 5′-ATCCTGGAC CCACTTCTTCTT-3’	This paper	N/A
Ccl24 forward primer: 5′-TCTTAGG GCCCTTCTTGGTG-3’	This paper	N/A
Ccl24 reverse primer: 5′-AATTCCAG AAAACCGAGTGG-3′	This paper	N/A
Il5 forward primer: 5′-CTCTGTTG ACAAGCAATGAGACG-3′	This paper	N/A
Il5 reverse primer: 5′-TCTTCAGT ATGTCTAGCCCCTG-3′	This paper	N/A
Il13 forward primer: 5′-CCTGGCTCTTGCTTGCCTT-3′	This paper	N/A
Il13 reverse primer: 5′-GGTCTTGT GTGATGTTGCTCA-3′	This paper	N/A
Gapdh forward primer: 5′-TTGATGG CAACAATCTCCAC-3′	This paper	N/A
Gapdh reverse primer: 5′-CGTCCC GTAGACAAAATGGT-3′	This paper	N/A
Software and Algorithms		
FlowJo	FlowJo	RRID: SCR_008520
PRISM	GraphPad	RRID: SCR_002798
ImageJ	Schneider et al., 2012	https://imagej.nih.gov/ij/
Imaris	BitPlane	RRID: SCR_007370
Cytobank	Cytobank	RRID: SCR_014043